Efficient in vitro and in vivo pulmonary delivery of nucleic acid by carbon dot-based nanocarriers

Philippe Pierrat, Rongrong Wang, Dimitri Kereselidze, Marie Lux, Pascal Didier, Antoine Kichler, Françoise Pons, Luc Lebeau

Efficient *in vitro* and *in vivo* pulmonary delivery of nucleic acid by carbon dot-based nano carriers

Philippe Pierrat,*[1] Rongrong Wang,[1] Dimitri Kereselidze,[1] Marie Lux,[1] Pascal Didier,[2] Antoine Kichler,[1] Françoise Pons,[1] and Luc Lebeau*[1]

[1] Laboratoire de Conception et Application de Molécules Bioactives, CNRS - Université de Strasbourg, Faculté de Pharmacie, 74 route du Rhin - BP 60024, 67401 Illkirch, France.

[2] Laboratoire de Biophotonique et Pharmacologie, CNRS - Université de Strasbourg, Faculté de Pharmacie, 74 route du Rhin - BP 60024, 67401 Illkirch, France.

Abstract

Cationic carbon dots were fabricated by pyrolysis of citric acid and bPEI25k under microwave radiation. Various nanoparticles were produced in a 20-30 % yield through straightforward modifications of the reaction parameters (stoichiometry of the reactants and energy supply regime). Particular attention was paid to the purification of the reaction products to ensure satisfactory elimination of the residual starting polyamine. Intrinsic properties of the particles (size, surface charge, photoluminescence and quantum yield) were measured and their ability to form stable complexes with nucleic acid was determined. Their potential to deliver plasmid DNA or small interfering RNA to various cell lines was investigated and compared to that of bPEI25k. The pDNA *in vitro* transfection efficiency of these carbon dots was similar to that of the parent PEI, as was their cytotoxicity. The higher cytotoxicity of bPEI25k/siRNA complexes when compared to that of the CD/siRNA complexes however had marked consequences on the gene silencing efficiency of the two carriers. These results are not fully consistent with those in some earlier reports on similar nanoparticles, revealing that toxicity of the carbon dots strongly depends on their protocol of fabrication. Finally, these carriers were evaluated for *in vivo* gene delivery through the non-invasive pulmonary route in mice. High transgene expression was obtained in the lung that was similar to that obtained with the golden standard formulation GL67A, but was associated with significantly lower toxicity. Post-functionalization of these carbon dots with PEG or targeting moieties should significantly broaden their scope and practical implications in improving their *in vivo* transfection efficiency and biocompatibility.

Efficient in vitro and in vivo pulmonary delivery of nucleic acid by carbon dot-based nanocarriers

Philippe Pierrat,*[1] Rongrong Wang,[1] Dimitri Kereselidze,[1] Marie Lux,[1] Pascal Didier,[2] Antoine Kichler,[1] Françoise Pons,[1] and Luc Lebeau*[1]

[1] Laboratoire de Conception et Application de Molécules Bioactives, CNRS - Université de Strasbourg, Faculté de Pharmacie, 74 route du Rhin - BP 60024, 67401 Illkirch, France.

[2] Laboratoire de Biophotonique et Pharmacologie, CNRS - Université de Strasbourg, Faculté de Pharmacie, 74 route du Rhin - BP 60024, 67401 Illkirch, France.

1. Introduction

Gene therapy is regarded as a promising treatment for many diseases, whether acquired (*e.g.* AIDS or cancer) or inherited through genetic disorder (cystic fibrosis, Parkinson's disease…). The basic concept underlying gene therapy is that disease may be treated by the transfer of genetic material into specific cells of a patient in order to enhance gene expression (DNA transfection) or to inhibit the production of a target protein by using the RNA interference machinery (*i.e.* siRNA transfection). Due to the size and the polyanionic nature of nucleic acid, its fragility towards nucleases, and the negative potential of the cell membrane surface, gene therapy requires the use of a proper carrier for safe and efficient intracellular delivery of the therapeutic payload. Though viral vectors offer greater efficiency of gene delivery, fundamental problems are associated with these carriers and many clinical trials in which they were used have been interrupted because of unexpected adverse effects [1-4]. Furthermore, severe limitations are encountered with respect to production and scale-up procedures. This has encouraged investigators to develop other potential scaffolds for introducing exogenous nucleic acids into targeted tissues. These so-called nonviral (or synthetic) carriers are typically based on cationic lipids or polymers, dendrimers, polypeptides, or solid nanoparticles, which can complex with negatively charged nucleic acid to form nano-sized particles [5]. Nonviral carriers have several advantages such as ease of synthesis, cell/tissue targeting, low immunogenicity and capacity to transport plasmid of unrestricted size. The most severe bottleneck in the clinical use of synthetic vectors is their low *in vivo* transfection efficiency and none of these vectors has received FDA or EMA approval to date. Therefore, efforts still are required for developing carriers allowing improved cell uptake, optimized endosome escape and migration of nucleic acid through the cytoplasm (to the cell nucleus or to the cytosolic RNA-induced silencing complex, RISC), together with dissociation of nucleic acid from the carrier for proper expression.

The recent discovery of carbon dots (CD) and the rapid advances in their synthetic preparation do offer a unique opportunity for investigating their potential as a new family of especially exciting carriers for nucleic acid delivery. These carbonaceous quantum dots combine several favorable attributes of traditional semiconductor-based quantum dots (namely, nanoscale size, size- and wavelength-dependent luminescence emission, resistance to photobleaching, ease of bioconjugation) without incurring the burden of intrinsic toxicity or elemental scarcity, and without the need for stringent, costly, or inefficient preparation steps [6]. Furthermore, CD surface passivation by amino compounds as required for obtaining exacerbated intrinsic fluorescence properties [7] allows straightforward installation of cationic charge density at the surface of the nanoparticles. This was investigated by Liu *et al.* who recently introduced polyethyleneimine (branched PEI 25 kDa, bPEI25k), a golden standard

transfection reagent (for recent reviews, see [8, 9]), for CD passivation [10]. The CD were prepared from bPEI25k and glycerol under microwave radiation. The resulting water-soluble brightly fluorescent nanoparticles exhibited *in vitro* DNA transfection efficiency comparable to control bPEI25k, with lower toxicity. These results are the very first to suggest the potential of CD for applications in gene delivery. Since then, only three other reports have described the use of engineered carbon dots for transfection purpose. In 2013, Kim *et al.* reported on a ternary complex between PEI-functionalized CD, PEI-functionalized gold nanoparticles and plasmid DNA (pDNA) for *in vitro* transfection and real-time monitoring of plasmid cellular trafficking [11]. In this study, the PEI-functionalized CD were prepared according to the procedure previously reported by Liu. More recently, Wu *et al.* described the hydrothermal preparation of CD by employing bPEI as carbon source [12]. The resulting cationic nanoparticles proved efficient for *in vitro* transfection of MCF-7 cells using EGFP as a reporter gene. Lastly, Chen *et al.* described the post-functionalization of CD with Alkyl-PEI2k (bPEI2k with 11 % of nitrogen atoms bearing a dodecyl substituent) and their use for *in vivo* delivery of DNA or siRNA [13]. Thus they demonstrated gene expression and silencing, respectively after intratumoral administration of CD-pDNA and CD-siRNA complexes in a xenografted tumor mouse model. Though the model used is a highly specific one, it provided the first proof of concept that CD can mediate transfection *in vivo*.

Herein, by employing citric acid and bPEI25k as carbon source, we established a simple and passivation-free route to cationic CD. The experimental conditions for the one-step pyrolysis of the carbon source under microwave radiation were systematically investigated. The as-produced carbon dots were purified by dialysis under specific conditions and did not require any post-functionalization for efficient DNA or siRNA *in vitro* transfection. The potential of these nanoparticles for *in vivo* DNA transfection by the non-invasive airway administration route was investigated.

2. Materials and methods

2.1. Materials

Citric acid was from Merck (Darmstadt, Germany). Branched PEI (MW 25kDa, bPEI25k) and 3-(4,5-dimethylthiazol-2-yl)-2,5-diphenyl tetrazolium bromide (MTT) were from Sigma-Aldrich (St Louis, MO, USA). Cholesterol (3-aminopropyl)[4-{(3-aminopropyl)amino}butyl] carbamate (GL67) was synthesized according to a described procedure [14]. DOPE (1,2-dioleoyl-sn-glycero-3-phosphoethanolamine) and DMPE-PEG_{5000} (1,2-dimyristoyl-sn-glycero-3-phosphoethanolamine-*N*-[methoxy (polyethyleneglycol)$_{5000}$]) were from Avanti Polar Lipids (Alabaster, Al, USA). To generate GL67A, the three lipids were formulated at 1:2:0.05 (GL67:DOPE:DMPE-PEG_{5000}) molar ratios [15]. Dialysis membranes were from Spectrum laboratories (Rancho Dominguez, CA, USA). A549 cells (human lung carcinoma; CCL-185), and NIH/3T3 cells (mouse embryo fibroblast; CRL-1658) were obtained from ATCC-LGC (Molsheim, France). pCMV-FLuc expression plasmid (5.5 kbp, BD Biosciences Clontech, Franklin Lakes, NJ, USA) was used as cytosolic luciferase reporter gene to monitor DNA transfection activity *in vitro* [16]. This plasmid encodes the *Firefly (Photinus pyralis) luciferase* gene under the control of a strong CMV promoter. To monitor DNA transfection *in vivo*, pCMV-GLuc (5.7 kbp, Nanolight Technologies, Pinetop, Az, USA) was used as luciferase reporter gene. This plasmid encodes the *Gaussia princeps luciferase* gene [17]. Cy5-labeled DNA (DNA-Cy5) was prepared from pCMV-GLuc and Cy5-*Label*IT reagent from Mirus Corp. (Madison, WI), following the manufacturer's instructions. The A549 cell line was transformed to stably express the *Photinus pyralis* luciferase gene originating from the pGL3 plasmid (Clontech, Mountain View, CA) to assess siRNA delivery [18, 19]. The pGL3 plasmid encoded as well for a gene conferring resistance to the antibiotic G418. This antibiotic was thus used to select the transfected A549-Luc cells. Luciferase gene silencing

experiments were performed with an RNA duplex (siLuc) of the sense sequence: 5'-CUU ACG CUG AGU ACU UCG A. Control untargeted RNA duplex (sic) was of sense sequence: 5'-CGU ACG CGG AAU ACU UCG A. Both RNAs as well as Cy5-labeled siLuc (siRNA-Cy5) were from Eurogentec (Angers, France). DNA concentration refers to phosphate content whereas siRNA concentration refers to duplex content. Fetal bovine serum (FBS), culture media (Dulbecco's Modified Eagle Medium, DMEM), Hank's Balanced Salt solution (HBSS), and supplements were from GIBCO-BRL (Cergy-Pontoise, France). Lysis and luciferin solutions for monitoring luciferase activity were purchased from Promega (Charbonnières, France). Coelenterazine was from Alfa Aesar (Bisheim, France). Eight-week-old male BALB/c mice were purchased from Charles River Laboratories (Saint-Germain-sur-l'Arbresle, France). They were housed in polycarbonate exhaust ventilated cages (M.I.C.E.® cages, Animal Care Systems) at a rate of 4 mice per cage, with bedding made from spruce wood chips (Safe, Villemoisson, France). Ventilation in the cages was set to 10-12 changes per hour, according to the manufacturer's recommendations. The animal room was maintained under controlled environmental conditions, with a temperature of 20 ± 2 °C, a relative humidity of 50 ± 10 % and a 12 h/12 h light/dark cycle (lighting 07:00-19:00). Food (standard diet 4RF21, Mucedola, Milan, Italy) and tap water were available *ad libitum*. The animals were acclimatized for 1 week before the initiation of the study. Animal experiments were performed in accordance with the European Union guidelines for use of laboratory animals and with the approval of the government body that regulates animal research in France (agreement number: AL/23/30/02/13).

2.2. Methods

Preparation of the CDs. The carbon dots were synthesized by microwave-assisted pyrolysis of citric acid. Briefly and unless otherwise stated, citric acid (0.50 g) was mixed with bPEI25k (0.25 g) in HCl 0.1 N (5 mL) in a 100 mL erlenmeyer flask. The homogeneous solution was submitted to microwave radiation in a 23 L domestic oven with a triple wave distribution system (TDS Silver ME82V, Samsung). Power output and reaction time were selected manually (typically, 700 W for 150 s). The reaction mixture was then cooled to room temperature, ultrapure water (5 mL) was added, and the resulting solution was centrifugated (5000 rpm, 5 min). The supernatant was loaded into a dialysis device (MWCO 3500 Da) and equilibrated against 500 mL HCl 0.1 N for 24 h (dialysate was replaced at 2, 6, and 12 h), and against ultrapure water for 48 h (dialysate was replaced once every 12 h). The residue was lyophilized to yield powdered material. Fourier transform infrared spectroscopy (FT-IR) was performed on a FT-IR Nicolet 380 spectrometer. NMR spectra were recorded on a Bruker 400 MHz Avance III instrument. ^{1}H- and ^{13}C-NMR chemical shifts δ are reported in ppm relative to internal reference (^{1}H: HDO at 4.78 ppm; ^{13}C in D_2O: $(\underline{C}H_3)_3COH$ at 30.83 ppm). The composition of the CDs was determined by elemental analysis on a Elementar Vario EL III apparatus.

Preparation of the CD-nucleic acid complexes. Procedure A: The DNA complexes formulated at various weight ratios for *in vitro* evaluations were prepared by mixing equal volumes of stock solutions of CD and pDNA (prepared at the adequate concentration in ultrapure water). The complexes were allowed to form for 30 min at room temperature without handling. Finally, the mixture was homogenized by pipetting up and down and subsequently used for *in vitro* transfection experiments. siRNA complexes were prepared similarly except that pure water was replaced by 150 mM NaCl. PEI/DNA and PEI/siRNA complexes were prepared similarly, from a 10 mM bPEI25k stock solution. Procedure B: The use of procedure A for the preparation of samples dedicated to *in vivo* experiments (final DNA concentration: 40 µg in 50 µL, *vide infra*) was troublesome at the lower CD/DNA

weight ratios (w/w < 2.1), resulting in heterogenous suspensions. To overcome this formulation problem, the complexes were prepared at low DNA concentration (typically 16 ng/µL) according to procedure A and were concentrated under reduced pressure at 30 °C in a SpeedVac concentrator apparatus for the appropriate time (typically 3 h). The final volume was adjusted with ultrapure water to set the DNA concentration at 40 µg in 50 µL.

Dynamic light scattering measurements. The average particle size and zeta potential (ζ) of CD-nucleic acid complexes were measured by DLS using a Zetasizer nanoZS apparatus (Malvern Instruments, Paris, France). All measurements were performed on freshly prepared complexes (*vide supra*) diluted in NaCl 1.5 mM, at 25 °C and in triplicate. Data were analyzed using the multimodal number distribution software supplied with the instrument and expressed as mean (± SD).

Transmission electron microscopy. Transmission electron micrographs were obtained using a benchtop TEM microscope (LVEM5, Cordouan Technologies, Pessac, France) operating at 5 kV. Carbon-coated grids (Cu-300HD, Pacific Grid Tech, San Francisco, USA) were glow discharged at 90 V and 3 mA for 20 s before deposition of the CD sample (10 µL, 10 µg/mL). After drying for 1 min, the grids were negatively stained with 2 % uranyl acetate (35 µL) for 20 s, and allowed to dry at room temperature for at least 2 h before observation.

UV-visible and fluorescence measurements. CD samples were prepared in ultra pure water (0.50 mg/mL). Spectra were recorded on a SAFAS Xenius XC spectrofluorimeter (SAFAS, Monaco) using a 1-mL quartz cuvette. Fluorescence spectra were recorded with excitation at 360 nm.

Quantum yield measurements. Quantum yields (Φ) were determined using quinine sulfate (qs) as standard ($\Phi_{qs} = 0.54$). The quantum yield of CD (in water) was calculated according to

$$\Phi_{CD} = \Phi_{qs} \cdot (F_{CD}/F_{qs}) \cdot (A_{qs}/A_{CD})$$

where Φ_{CD} and Φ_{qs} were the quantum yields for CD and quinine sulfate (resp.), F_{CD} and F_{qs} were the measured integrated emission intensities, and A_{CD} and A_{qs} were the absorbances. In order to minimize fluorescence quenching, absorbance in the 10 mm fluorescence cuvette was kept below 0.10 at the excitation wavelength (360 nm).

Nucleic acid retardation assay. Freshly prepared CD-nucleic acid complexes at the desired w/w ratio were analyzed by electrophoresis through a 1 % agarose gel. The gel was run in a 40 mM Tris-acetate-EDTA buffer, pH 8.0 (TAE) and DNA or siRNA was stained using an ethidium bromide solution (EB, 0.5 µg/mL).

Cell culture. All cell lines were grown in culture flasks at 37 °C in a 5 % CO_2 humidified chamber. A549 cells were grown in DMEM-F12 medium containing FBS (10 %), L-glutamine (2 mM), penicillin (100 units/mL), streptomycin (100 µg/mL), and Hepes (5mM). A549-Luc cells were grown in RPMI 1640 supplemented with FBS (10 %), L-glutamine (2 mM), penicillin (100 units/mL), and streptomycin (100 µg/mL). Selection of A549-Luc cells was done by the addition of G418 (0.8 mg/mL) to the culture medium. At confluence, cells were released with trypsin, centrifuged (4 °C, 5 min, 120 g), resuspended in culture medium, and counted before seeding in culture flasks (subculturing) or plates (transfection experiment).

Cell imaging. For confocal laser scanning microscopy, A549 cells were seeded into 8-well IbiTreat µ-slides (Ibidi) at a density of 27,000 cells/well in 300 µL complete culture medium 24 h before use. The culture medium was replaced by 270 µL fresh medium and the CD/DNA or CD/siRNA complexes (30 µL) were added. Cells were incubated for the indicated amount

of time in a 5 % CO_2 humidified chamber. Then the culture medium was removed, cells were washed with serum-free culture medium (500 µL), and 300 µL NR12S fluorescent probe (10 nM in HBSS) were added [20]. The samples were examined under a Leica SPE confocal laser scanning microscope equipped with four laser sources (405, 488, 561, and 635 nm).

In vitro DNA transfection. A549 cells were seeded into 96-well culture plates (Becton-Dickinson) at a density of 6,000 cells/well in 100 µL complete culture medium. Twenty-four hours later, freshly prepared CD/pCMV-FLuc complexes (typically 12.5 µL, *i.e.* 0.2 µg pDNA) were added to each well of the plates. Then, cells were let to grow in the incubator without further handling for 24 h, before *Firefly* luciferase gene expression assessment.

In vitro siRNA transfection.
A549-Luc cells were seeded into 48-well culture at a density of 22,000 cells/well in 500 µL complete culture medium. Twenty-four h later, cell confluency was around 50 %. Complete culture medium was replaced by serum-free medium and freshly prepared CD/siRNA complexes (250 µL, *i.e.* 167 ng sic or siLuc) were added to each well of the plates (final siRNA concentration: 50 nM). After 3 h of incubation, medium was replaced with serum-supplemented fresh one. Then, cells were let to grow in the incubator without further handling for 48 h, before *Firefly* luciferase gene expression assessment. Protein content/well was determined using a Bradford assay (Bio-Rad).

In vivo transfection. The CD/DNA complexes (40 µg pCMV-GLuc) prepared at the adequate w/w ratio in water (50 µL) were administered as a single dose into the lung of mice by intranasal instillation. Control animals received instillation of the same volume of water. Intranasal instillation was used, as it is noninvasive, effective in delivering substances into the lung of mice and reproducible [21]. It was carried out under light anesthesia with 50 mg/kg ketamine (Imalgen®, Merial, Lyon, France) and 3.33 mg/kg xylazine (Rompun®, Bayer, Puteaux, France) given i.p. The experiment was terminated at 24 h by i.p. injection of ketamine (150 mg/kg) and xylazine (10 mg/kg). The trachea was cannulated to perform bronchoalveolar lavages. Lungs were lavaged by 2 instillations of 0.5 mL ice-cold saline supplemented with 2.6 mM EDTA (saline-EDTA). Bronchoalveolar lavage fluids (BALF) were centrifuged (200 x g for 5 min at 4 °C), and the resulting supernatant was stored at -20 °C until cytokine measurements. After thoracotomy, lungs were perfused *in situ* through the pulmonary artery with 10 mL of ice-cold PBS, collected, and frozen in liquid nitrogen, and stored at -80 °C until assessment of the *Gaussia* luciferase gene expression.

Firefly luciferase assay. *Firefly* luciferase gene expression was determined in transfected cells using a commercial kit (Promega, Charbonnières, France) with slight modifications compared to the manufacturer's recommendations as described elsewhere [22]. Briefly, at the end of the transfection experiments, the cell culture medium was carefully removed. The adherent cells were washed with PBS (100 and 600 µL for pDNA and siRNA transfection, respectively) and treated with the kit lysis buffer (20 and 100 µL for pDNA and siRNA transfection, respectively) for 15 min. The resulting lysate was diluted with PBS (150 µL for pDNA transfection; no dilution in the case of siRNA transfection in 48-well plates) before luciferase assessment. Luciferase content was measured on an aliquot of lysate (5 µL) by monitoring light production for 1 sec after addition of the luciferin substrate (35 µL) using a luminometer (Berthold Centro LB960 XS, Thoiry, France). Value for each sample is the mean of a triplicate determination (± SD).

Gaussia luciferase assay. *Gaussia* luciferase gene expression was assessed in mouse lung homogenates. Frozen lungs were homogenized in 600 µL of PBS containing a protease inhibitor cocktail (Complete EDTA-free tablets, Roche, Germany), using an Ultra-Turrax®

homogenizer (T25, Ika, Staufen, Germany). After a 20-min incubation on ice, the homogenates were transferred into Qiashredder columns (Qiagen, Courtabœuf, France) and centrifuged at 13,000 g for 1 min. Columns were then removed and the homogenates were centrifuged for an additional 5-min period. The supernatants were collected, protein content was determined using a Bradford assay (Bio-Rad), and *Gaussia* luciferase content was measured by monitoring light production on an aliquot of sample (10 µL) for 1 sec upon addition of the coelenterazine substrate (50 µL). Value for each sample is the mean of a triplicate determination (± SD).

Cytotoxicity assays. Mitochondrial activity (MTT assay) and/or lactate dehydrogenase release (LDH assay) measurements were used to assess the cytotoxicity of CD/nucleic acid complexes upon transfection experiments, and to carry out thorough toxicity evaluations on selected CD. For MTT assay, at the end of cell treatment, culture medium was removed and cells were carefully washed with PBS. Complete culture medium containing 0.5 mg/mL MTT was added to the cells (100 µL/well) that were incubated for 2 h at 37 °C. Then culture medium was removed and cells were lysed with DMSO (70 µL). Intensity of MTT reduction was evaluated by measuring absorbance of the resulting solution at 570 nm. Viability of treated cells was expressed as the percentage of the absorbance measured in untreated cells. Value for each sample is the mean of triplicate determinations (± SD). For LDH assay, at the end of cell treatment, an aliquot of supernatant (100 µL) was transferred into a 96-well assay plate and LDH activity was measured using a commercial kit (Cytotoxicity Detection Kit Plus, Roche Applied Science) according to the manufacturer's instructions. LDH activity was expressed as the percentage of the maximal LDH release obtained after lysis of untreated cells. Value for each sample is the mean of a triplicate determination (± SD). LDH release values of less than 10 % were considered as non-significant.

Cytokine assay. Keratinocyte-derived chemokine (KC) was measured in bronchoalveolar lavage fluids by ELISA according to the manufacturer's instructions (BD Biosciences, Le Pont de Claix, France). Value for each sample is the mean of a triplicate determination (± SD).

3. Results and discussion

3.1. CDs preparation and characterization

C-dots can be produced inexpensively by many approaches (arc discharge, laser-ablation, electrochemistry, combustion, solvothermal heating) [23]. Of special interest are the methods involving microwave pyrolysis of hydrophilic carbon sources (glycerol, citric acid, glucose, chitosan…) [7, 24-34]. We selected citric acid (CA) as the carbon source and used bPEI25k for *in situ* passivation. As CD homogeneity and purity is an issue for their further biological applications, we first set up and validated a purification protocol ensuring satisfactory elimination of residual starting material, *i.e.* bPEI25k. As the most usual technique to purify CD is dialysis, we first examined dialysis of a mixture of citric acid and bPEI25k that was not exposed to microwave radiation. Dialysis were conducted with a 3500 Da cut-off membrane, under various pH conditions. At the end of the dialysis process, the sample was removed from the dialysis bag and lyophilized, and the dry residue was weighted. Whatever the pH value, starting material could not be quantitatively removed, even after prolonged dialysis (table 1). Under neutral dialysis conditions, 22.3 % of material (in weight) was recovered at the end of the dialysis. As might be expected, this material was identified as the citrate salt of PEI (determined by ^{1}H-NMR, data not shown) and represented *ca.* 28 % of the initial amount of PEI. Better results were obtained either under highly acidic or basic dialysis conditions with 5-6 % residue, *i.e.* 10 % of starting PEI (hydrochloric salt obtained under acidic dialysis). As most of the CD purifications by dialysis reported in the literature involved a 1.000 Da MWCO

membrane, we examined dialysis on such a lower cut-off membrane as well. The results revealed that 27.9 % of material was recovered at the end of the dialysis carried out at pH 7, representing *ca.* 35 % of the initial amount of PEI. This amount was lowered to 9.1 % (15 % of the initial amount of PEI) when dialysis was carried out at pH 1. These results thus revealed that standard dialysis conditions as described in most of the previously reported preparations of PEI-passivated CD can't efficiently remove unreacted PEI from the reaction mixture. Using a dialysis membrane with a higher molecular weight cut-off (10 kDa) only slightly improved PEI elimination but most probably would lead to excessive loss of CD (*vide infra*). Though not fully satisfactory and with respect to the target application requiring a polycationic species, dialysis under acidic conditions (pH 1) with a 3500 Da cut-off membrane was retained as an acceptable compromise for CD purification and was used in the following.

Table 1

Considering the synthesis of the nanoparticles, we first looked at the influence of pH on the properties of those formed from CA and bPEI25k under microwave radiation. We thus performed pyrolysis at various pH and measured the size, zeta potential, and fluorescence of the resulting CD after purification by dialysis (table 2). The smaller particles were obtained under acidic conditions, and fluorescence intensity decreased with increasing particle size which is consistent with previously reported data [35, 36]. With regard to the charge of the nanoparticles, those prepared at *ca.* neutral pH exhibited a zeta potential value (ζ) close to zero though purification was carried out at pH 1. This likely indicates that there was low density of ammonium groups at the surface of these dots. Irradiation under acidic conditions provided highly positively charged nanoparticles. Based on particle size and fluorescence of the nanoparticles produced, all subsequent fabrications of CD where realized under microwave radiation at pH 1.

Table 2

The energy supply during pyrolysis was expected to influence characteristics of the CD. We thus first proceeded to pyrolysis at a fixed oven power output (700 W), and measured the size of the particles over time (fig. 1). Nanoparticles were detected by DLS after 60 s irradiation, with a mean size of pristine material of *ca.* 1.2 nm. That size increased more and more rapidly to reach 3.5 nm after 150 s, and 9.2 nm after 180 s. With longer irradiation time, increasing amount of insoluble dark material was observed upon dispersion in water. It is worth noting that the aqueous solutions of the pristine CD were highly fluorescent and that the size measured for the nanoparticles was typically in the range 2-10 nm. After dialysis of the samples on a 3500 Da cut-off membrane, their titrated solutions were less fluorescent whereas the particle size measured by DLS was significantly increased (10-20 nm). The decrease of the fluorescence intensity of the samples after dialysis may be attributed to the loss of the brighter nanoparticles, *i.e.* the smaller ones, through the membrane. With respect to the size of the nanoparticles, dialysis against HCl 0.1 N results in extensive protonation of the amine groups, which improves electrostatic repulsions between the polycationic chains and thus provokes particle swelling.

Figure 1

In another set of experiments, we modified the energy supply regime of the microwave oven. The amount of energy thus delivered to the samples was rigorously the same (29.17 W.h, *i.e.*, 105 kJ) but apparatus power output and irradiation time were varied. The particles produced were analyzed after dialysis and characterized using various methods (table 3, table S1, fig. S1-S3). All the carbon dots prepared under these conditions were highly positively charged and their size was homogeneous (12.0-13.2 nm), except for **CD-7**, thoses for which the higher microwave power was supplied for the shorter period of time and which size was significantly larger (19.7 nm). Thus varying the regime of microwave supply appeared as a convenient mean for tuning the size of the CD. Regardless of their size, strong fluorescence of the dots likely involved high pyrolysis temperature since the brighter nanoparticles were obtained through the shorter activation processes. Considering the quantum yield of the CD, relatively high values were obtained (31.5-48.1 %), and may be compared to those previously reported in the literature for PEI-passivated CD (7-15 % [10]; 54.3 % [12]).

Table 3

The influence of stoichiometry of CA and PEI on the properties of the CD that were produced was investigated as well (table 4). The data show no clear trend with respect to the size and charge of the nanoparticles as the purified CD all were highly positively charged (+ 42.1 to + 61.5 mV) and of similar size (19.7 to 24.9 nm). At the opposite, the photoluminescence properties clearly showed a marked dependence on the stoichiometry of the reactants. Thus increasing the amount of cationic polymer in the reaction mixture resulted in a decreased brigthness of the CD produced, by *ca.* an order of magnitude, and quantum yield was reduced from 35 to 28 %. On the other hand, elemental analysis (hydrogen, carbon, and nitrogen content) of the CDs revealed only slight differences (table SI-1) and it has not been possible to establish any correlation with the nanoparticle properties.

Table 4

Carbon dots **CD-4** to **CD-9** were examined by transmission electron microscopy (fig. 2) and the size of the nanoparticles observed was found to be in good agreement with those determined by DLS (inset).

Figure 2

Figure 3

The optical properties of the CD prepared under the various experimental conditions have been further examined in detail. First, with none of the samples investigated herein did we observe the λ_{exc}-dependence of the emission wavelength that is usually described with CD [23]. As an example, figure 3 shows the photoluminescence spectra recorded for **CD-7** with incremented excitation wavelengths from 300 to 410 nm. Normalized luminescence emissions (see inset) revealed that there was no emission peak shift when excitation was performed in the range 300-390 nm. Only at the higher excitation wavelenths a small blue shift (400: $\Delta\nu = 4$ nm, 410: $\Delta\nu = 8$ nm) was observed, when luminescence intensity became very low.

Full absorbance and photoluminescence spectra for **CD-4** to **CD-9** are presented in figure 4. Whatever the experimental conditions used for the production of the nanoparticles, the strong optical absorption in the UV region did not significantly change with respect to the absorption wavelength (λ_{abs} = 356-359 nm). This was also the case for the luminescence emission (λ_{em} = 442 nm), except for **CD-9** which emission peak was red-shifted by 10 nm. At the opposite, significant differences were observed with respect to the optical density and photoluminescence intensity of the nanoparticles, as already mentioned above. For the same initial composition of the reaction mixture, absorbance of the CD was maximized with the shorter microwave irradiation time (**CD-7**). Variation of the CA/PEI ratio as well proved to be critical. The optical density of the CD prepared under the same microwave irradiation regime was improved by a *ca.* eigth-fold factor when decreasing the amount of bPEI25k in the reaction mixture from 50 to 20 % (w/w). The brightness of the nanoparticles followed a similar trend. Thus roughly linear relationships could be established between the absorbance and brightness of the CD, and the microwave irradiation time, provided the same amount of energy was delivered to the sample (**CD-4** to **CD-7** series). At the opposite, no such correlation did appear in the CD series in which the stoichiometry of the reactants was varied (**CD-7** to **CD-9**).

Figure 4

Before examining the potential for the various nanoparticles to mediate nucleic acid delivery into cells, their capacity to form complexes with pDNA has been determined by an agarose gel retardation assay (fig. 5). The assay has been conducted with increasing CD/DNA w/w ratios. DNA retardation was observed with all the CD assayed. However it occured at various w/w ratios depending on the parameters of nanoparticle fabrication. Considering the **CD-4** to **CD-7** series, it did clearly appear that the energy supply regime had a significant impact on the nucleic acid complexation ability of the dots. Semi-quantitative analysis of the electrophoretic patterns showed that **CD-4** more efficiently complexed DNA than **CD-5**, which was followed by **CD-6**, and **CD-7**. These observations quite made sense as it may be expected that the higher the positive zeta potential of the dots, the lower is the quantity required for neutralization of the polyanionic DNA. This also revealed that at low irradiation regime, PEI molecules involved in the formation of the dots were pyrolyzed to a lesser extent than at high regime, and titrable nitrogen centers were better preserved. The data corresponding to the series of dots in which the amount of PEI was varied (**CD-7**, **CD-8**, and **CD-9**) could not be interpreted in the same way. Indeed it was rather the amount of PEI involved in the preparation of the dots that seemed to condition DNA complexation. Thus the CD prepared with 50 % PEI (**CD-9**) more efficiently condensed DNA than those prepared with 33 % PEI (**CD-7**), which were better than **CD-8** (20 % PEI). Though this makes perfect sense, the reason why the ζ values measured in this series of dots do not fit the same progression is not understood (*vide supra*). To tentatively go a step further in our understanding of the properties of the dot-DNA complexes, we determined the size and ζ for the complexes obtained with **CD-7** (table 5). The data revealed that the size of the complexes homogeneously decreased when the CD/DNA weight ratio was increased. Though this is consistent with the DNA condensation process, one might have expected a significant change in the size of the complexes at the higher w/w ratios with respect to that of the "bare" carbon nanoparticles. This was not the case (20.6 ± 3.5 nm and 19.7 ± 1.1 nm for **CD-7**/DNA w/w 32 and **CD-7**, respectively) and might find a possible explanation in the neutralization of the repulsive interactions between the polyamonium chains at the periphery of the particles by the polyanionic DNA, thus reversing the nanoparticles swelling that was observed under acidic

conditions (*vide supra*). Considering the charge of the particles, the ζ values steadily increased with the w/w ratio.

Table 5

3.2. *In vitro* evaluation of the carbon dots

3.2.1. DNA transfection

Based on their properties (intrinsic fluorescence, size, and ζ potential), **CD-4**, **CD-7**, and **CD-8** were selected for *in vitro* evaluation. The ability of these CD to promote pDNA delivery into cells was determined by measuring the level of transgene expression in the A549 lung epithelial cell line after a 24-h incubation period with the CD/pCMV-FLuc complexes (fig. 5). For comparison, the golden standard transfection reagent bPEI25k was examined in parallel. All the carriers displayed rather similar transfection profiles (fig. 5, left). The higher transfection rate with the CD as carriers however required a larger amount of DNA than with bPEI25k (0.8 *vs.* 0.4 µg/mL). Yet the more efficient transfection conditions involved **CD-7** (0.8 µg DNA, w/w 2) which outperformed bPEI25k (0.4 µg DNA, w/w 2) by a *ca.* two-fold factor. Besides, **CD-4**, **CD-7**, and bPEI25K all three displayed optimum efficacy for a carrier/DNA weight ratio close to 2. In the case of **CD-8**, high transfection efficiency was only achieved with a significantly higher w/w ratio (*i.e.* 8-16). With the CD as nucleic acid carriers, the transfection rate was improved with increasing DNA concentration. Though this could make sense, it is worth to note that the opposite was observed with bPEI25k. This discrepancy is not understood and cannot be explained on the basis of the toxicity profile of the carriers, as measured by LDH release, as these profiles quite well superimpose one to another (fig. 5, right). Once again, the only significant difference was observed with **CD-8** for which cytotoxicity was only detected at the higher w/w ratios. Finally, the transfection efficiency of bPEI25K and PEI-based CD was found to be rather equivalent except bPEI25k was efficient at lower DNA concentrations and **CD-7** achieved a higher transfection rate.

Figure 5

In order to address the toxicity issue in more detail, we determined the cell viability by MTT assay and the cytotoxicity by LDH release upon exposure of A549 cells for 24 h to an escalating dose of **CD-7** and its complex with pDNA. For comparison, bPEI25k and the corresponding polyplexes were evaluated as well. In both assays, bPEI25k revealed more harmful to the cells than the PEI-based CD by a *ca.* two-fold factor (fig. 6a, b). With respect to the toxicity of the **CD-7**/DNA and bPEI25k/DNA complexes, the same trend was observed. This was the case with another cell line investigated (NIH-3T3, fig. S5). The complex **CD-7**/DNA was assayed at a w/w ratio of 2.6 (selected from *in vitro* experiments, data not shown), whereas the bPEI25k/DNA polyplex was assayed at a w/w ratio of 1.3. This corresponds to a charge ratio N/P of 10 (where N is the concentration of PEI amine and P that of nucleic acid phosphate) that has been previously determined for optimized *in vivo* transfection (*vide infra*). Our results are consistent with those in previous reports [10, 12] though the cytotoxicity associated with **CD-7** and **CD-7**/DNA complexes was found significantly higher than that claimed for the CD prepared by Liu *et al.* from bPEI25k in glycerol, and for their complexes with DNA [10]. Most recent results reported for pristine CD obtained *via* hydrothermal

treatment of chitosan, PEI and acetic acid in water [37] or of maltose and PEI [38] are along the same line which suggests that the toxicity of CD strongly depends on the fabrication conditions.

Figure 6

3.2.2. siRNA transfection

In order to evaluate the ability of **CD-7** to deliver small interfering RNA *in vitro*, A549-Luc cells were transfected with *Firefly* luciferase targeted siRNA and gene expression was assessed by monitoring enzyme activity (fig. 7). An efficient silencing of the Luciferase gene was observed with **CD-7**. Hence, a 55 % specific gene silencing was obtained at a CD/siRNA weight ratio of 12, and a 85 % gene knockdown was achieved for w/w ratios in the range 50-100. For the higher ratios however, significant toxicity occurred which resulted in a sharp increase of non-specific silencing and decreased cell viability (data not shown). This result was fully consistent with those obtained in the previously discussed toxicity studies conducted with **CD-7**/DNA complexes (fig. 6). Besides, the more pronounced cytotoxicity of bPEI25k when compared to **CD-7** (*vide supra*) had a marked effect on the siRNA transfection efficiency and high level-specific gene silencing (> 70 %) could not be achieved without provoking significant non-specific silencing.

Figure 7

3.2.3. Cell imaging

Cellular trafficking and dissociation of the CD/nucleic acid molecular assemblies was further investigated using confocal laser scanning fluorescence microscopy. A549 cells incubated with **CD-7**/DNA-Cy5 were observed at different time points (fig. 8). For convenience, the cell membrane was labelled with the NR12S fluorescent probe [20]. After 1 h incubation, the CD fluorescence (blue) was massively found in the cells and cellular uptake increased with time. It is worth to note that punctuated DNA-Cy5 fluorescence (red) could only be detected outside the cells, co-localizing with CD and presumably due to residual membrane-bound complexes that resisted the washing step. This suggests that **CD-7**/DNA-Cy5 complexes rapidly disassembled once inside cells and that released individual DNA molecules had too weak fluorescence emission to be properly detected with our instrument. The same experiment was conducted with **CD-7**/siRNA-Cy5 assemblies (fig. 9). Again the complexes were rapidly internalized and after 1 h incubation both CD and siRNA were easily visualized in the cells. The amount of siRNA in the cell compartments increased with time, a part of it being involved in complexes with the CD (d, pink), and another one being clearly dissociated from the nanoparticles (d, red).

Figure 8

Figure 9

3.2. *In vivo* evaluation of **CD-7**

Many nucleic acid carriers that are efficient to transfect cells *in vitro* fail to function or display serious toxicity *in vivo*. To the best of our knowledge, there is only one report up to date describing the *in vivo* delivery of nucleic acid with CD [13]. In this study, the nanocomplexes were directly injected into tumor tissues in a xenografted tumor mouse model. Interested in investigating a non-invasive administration route for *in vivo* gene delivery and in targeting lung diseases, we evaluated the transfection ability of **CD-7** after local delivery of pCMV-GLuc to the lung of BALB/c mice by intranasal administration. The *Gaussia princeps* luciferase expression plasmid was preferred to that of *Photinus pyralis* as it is a more sensitive reporter gene which is particularly useful for monitoring airway gene transfer [15]. A number of lung gene delivery systems have been described in the literature [39-41]. For comparison purpose, we thus selected two golden standard transfection reagents for gene delivery to the lung, bPEI25k and the cationic lipid formulation GL67A, that were evaluated in parallel with **CD-7** (fig. 10). Branched PEI25k was assayed in the optimized conditions as previously described for DNA delivery to the lung, *i.e.* with a charge ratio N/P = 10 (corresponding to w/w = 1.3) [42, 43]. Similarly, GL67A/DNA formulations were prepared at N/P = 0.75, as was extensively validated in previous pre-clinical and clinical evaluations [14, 44-46]. Results indicated that **CD-7** afforded similar *in vivo* transfection efficiency as the golden standard GL67A formulation, and was significantly more efficient than bPEI25k. As the standard procedure (*i.e.* protocol A, see Materials and methods section) to prepare CD/DNA complexes with low w/w ratios at the high concentration required for *in vivo* testing revealed troublesome and furnished heterogenous suspensions, we got around through performing post-concentration of diluted samples (protocol B). In this way, small transfection particles were obtained (48-57 nm) that were expected to outperform the larger ones produced *via* the conventional procedure (190-200 nm) (table 6). Indeed, the reported mesh-pore size range in mucus is 20-200 nm [47, 48], and large particles are sought to undergo slower diffusional transport through mucus barriers or not even are they capable of crossing mucosal barriers. Our results did not support this general view, since the small particles prepared according to protocol B revealed significantly less efficient than the larger ones. Considering those particles with a weight ratio of 2.6, transfection efficiency achieved with the small **CD-7**/DNA complexes (48.6 ± 0.3 nm) was decreased by a four-fold factor when compared to the large ones (205.3 ± 30.6 nm). One possible explanation for this may be found in the work by Hanes *et al.* on respiratory mucus that may be compared to a size-exclusion chromatography matrix [49]. According to this, in a network with heterogenous pore size, small particles can access a greater number of small pores or pockets in the gel, resulting in an overall reduced transport rate over long distance. *In vivo*, the mucus gel layer sits atop the periciliary layer, which is expected to serve as a further barrier to particles. To efficiently reach the target cells, nanoparticles hence have to diffuse through the mucus to the periciliary layer faster than it is swept by mucociliary activity [50]. Consequently, retardation of the small (transfection) particles getting lost in the smaller pores and pockets in the mucus gel favors their elimination by mucociliary clearance whereas larger particles move more rapidly towards the periciliary layer and get past the first hurdle on their journey to the target cells.

Figure 10

Table 6

Finally, to gain insight into the *in vivo* toxicity of the CD/DNA nanoparticles, airway inflammation was assessed by measuring levels of keratinocyte-derived chemokine (KC) in the bronchoalveolar lavage fluids (BALF) of treated mice (fig. 11). The results indicate that the DNA complexes with **CD-7** provoked less severe inflammation than those with the reference delivery systems GL67A or bPEI25k. For the more efficient formulation in transfection, *i.e.* **CD-7**/DNA with a w/w ratio of 2.6, the cytokine concentration established at 111.9 pg/mL, whereas it was increased to 191.3 pg/mL (*i.e.* + 71 %) with GL67A, and to 125.4 pg/mL (*i.e.* + 12 %) with bPEI25k.

Figure 11

Thus the transfection efficiency achieved with **CD-7**/DNA at a w/w ratio of 2.6 favorably compared with that achieved with GL67A/DNA. Furthermore these nanoparticles were better tolerated *in vivo*. This is not without significance as GL67A is a PEGylated carrier whereas **CD-7** is not, thereby opening interesting avenues for further development of CDs as *in vivo* gene delivery vehicles. Indeed PEGylation of gene transfer reagents proved a successful tool for significant improvement of *in vivo* transfection efficiency and safety [51, 52].

4. Conclusion

In summary, we have developed a straightforward and unexpensive method to prepare cationic carbon dots by one-step microwave assisted pyrolysis of citric acid in the presence of branched PEI 25 kDa. Preparations were performed in the gram-scale and can be easily scaled up. Special attention was paid to purifying the nanoparticles that were obtained with respect to subsequent *in vitro* and *in vivo* experimentations. The quantum yield of the particles was calculated to be in the range 31.5-48.1 % which corresponds to the high values reported to date for such particles. The as-prepared cationic nanoparticles proved efficient for condensing DNA, and the size of the resulting complexes could be tuned depending on the complexation protocol that was carried out. *In vitro*, the complexes with DNA were shown to transfect cells with a similar efficiency to that of bPEI25k, and a reduced toxicity. The carbon nanoparticles proved efficient as well for siRNA delivery to cells and high specific gene knockdown was achieved without associated cytotoxicity, contrary to what was observed with bPEI25k. Finally, non-invasive administration of CD/DNA to mouse lungs demonstrated that these new carriers achieved similar efficiency to that of GL67A, the golden standard formulation for pulmonary administration of DNA, with lower toxicity. Opportunities for post-functionalization of these nanoparticles with PEG or targeting moieties should significantly broaden their scope and practical implications in improving their *in vivo* biocompatibility.

Acknowledgements

We wish to thank Anne Casset and Salif Ali for technical assistance.

Efficient in vitro and in vivo pulmonary delivery of nucleic acid by carbon dot-based nanocarriers

Philippe Pierrat, Rongrong Wang, Dimitri Kereselidze, Marie Lux, Pascal Didier, Antoine Kichler, Françoise Pons, and Luc Lebeau

References

[1] Marshall E. Gene therapy death prompts review of adenovirus vector. Science 1999;286:2244-5.

[2] Hacein-Bey-Abina S, von Kalle C, Schmidt M, Le Deist F, Wulffraat N, McIntyre E, et al. A serious adverse event after successful gene therapy for X-linked severe combined immunodeficiency. New Engl J Med 2003;348:255-6.

[3] Baum C, Dullmann J, Li ZX, Fehse B, Meyer J, Williams DA, et al. Side effects of retroviral gene transfer into hematopoietic stem cells. Blood 2003;101:2099-114.

[4] Sakurai H, Kawabata K, Sakurai F, Nakagawa S, Mizuguchi H. Innate immune response induced by gene delivery vectors. Int J Pharm 2008;354:9-15.

[5] Mintzer MA, Simanek EE. Nonviral vectors for gene delivery. Chem Rev 2009;109:259-302.

[6] Ding CQ, Zhu AW, Tian Y. Functional surface engineering of C-Dots for fluorescent biosensing and in vivo bioimaging. Acc Chem Res 2014;47:20-30.

[7] Liu CJ, Zhang P, Tian F, Li WC, Li F, Liu WG. One-step synthesis of surface passivated carbon nanodots by microwave assisted pyrolysis for enhanced multicolor photoluminescence and bioimaging. J Mater Chem 2011;21:13163-7.

[8] Di Gioia S, Rejman J, Carrabino S, De Fino I, Rudolph C, Doherty A, et al. Role of biophysical parameters on ex vivo and in vivo gene transfer to the airway epithelium by polyethylenimine/albumin complexes. Biomacromolecules 2008;9:859-66.

[9] Neuberg P, Kichler A. Recent developments in nucleic acid delivery with polyethylenimines. In: Huang L, editor. Non-viral vectors for gene therapy: Lipid- and polymer-based gene transfer. Academic Press, 2014. p. 263–288.

[10] Liu C, Zhang P, Zhai X, Tian F, Li W, Yang J, et al. Nano-carrier for gene delivery and bioimaging based on carbon dots with PEI-passivation enhanced fluorescence. Biomaterials 2012;33:3604-13.

[11] Kim J, Park J, Kim H, Singha K, Kim WJ. Transfection and intracellular trafficking properties of carbon dot-gold nanoparticle molecular assembly conjugated with PEI-pDNA. Biomaterials 2013;34:7168-80.

[12] Hu LM, Sun Y, Li SL, Wang XL, Hu KL, Wang LR, et al. Multifunctional carbon dots with high quantum yield for imaging and gene delivery. Carbon 2014;67:508-13.

[13] Wang L, Wang X, Bhirde A, Cao J, Zeng Y, Huang X, et al. Carbon-dots-based two-photon visible nanocarriers for safe and highly efficient delivery of siRNA and DNA. Adv Healthcare Mater 2014;3:1203-9.

[14] Lee ER, Marshall J, Siegel CS, Jiang CW, Yew NS, Nichols MR, et al. Detailed analysis of structures and formulations of cationic lipids for efficient gene transfer to the lung. Hum Gene Ther 1996;7:1701-17.

[15] Griesenbach U, Vicente CC, Roberts MJ, Meng CX, Soussi S, Xenariou S, et al. Secreted Gaussia luciferase as a sensitive reporter gene for in vivo and ex vivo studies of airway gene transfer. Biomaterials 2011;32:2614-24.

[16] Zanta MA, Boussif O, Adib A, Behr JP. In vitro gene delivery to hepatocytes with galactosylated polyethylenimine. Bioconjugate Chem 1997;8:839-44.

[17] Tannous BA. Gaussia luciferase reporter assay for monitoring biological processes in culture and in vivo. Nat Protoc 2009;4:582-91.
[18] Dikmen ZG, Gellert GC, Jackson S, Gryaznov S, Tressler R, Dogan P, et al. In vivo inhibition of lung cancer by GRN163L: a novel human telomerase inhibitor. Cancer Res 2005;65:7866-73.
[19] Foillard S, Zuber G, Doris E. Polyethylenimine-carbon nanotube nanohybrids for siRNA-mediated gene silencing at cellular level. Nanoscale 2011;3:1461-4.
[20] Kucherak OA, Oncul S, Darwich Z, Yushchenko DA, Arntz Y, Didier P, et al. Switchable Nile Red-based probe for cholesterol and lipid order at the outer leaflet of biomembranes. J Am Chem Soc 2010; 132:4907-16.
[21] Ronzani C, Spiegelhalter C, Vonesch JL, Lebeau L, Pons F. Lung deposition and toxicological responses evoked by multi-walled carbon nanotubes dispersed in a synthetic lung surfactant in the mouse. Arch Toxicol 2012;86:137-49.
[22] Pierrat P, Kereselidze D, Wehrung P, Zuber G, Pons F, Lebeau L. Bioresponsive deciduous-charge amphiphiles for liposomal delivery of DNA and siRNA. Pharm Res 2013;30:1362-79.
[23] Baker SN, Baker GA. Luminescent carbon nanodots: Emergent nanolights. Angew Chem-Int Ed 2010;49:6726-44.
[24] Zhu H, Wang XL, Li YL, Wang ZJ, Yang F, Yang XR. Microwave synthesis of fluorescent carbon nanoparticles with electrochemiluminescence properties. Chem Commun 2009:5118-20.
[25] Chandra S, Das P, Bag S, Laha D, Pramanik P. Synthesis, functionalization and bioimaging applications of highly fluorescent carbon nanoparticles. Nanoscale 2011;3:1533-40.
[26] Wang QL, Zheng HZ, Long YJ, Zhang LY, Gao M, Bai WJ. Microwave-hydrothermal synthesis of fluorescent carbon dots from graphite oxide. Carbon 2011;49:3134-40.
[27] Zhai XY, Zhang P, Liu CJ, Bai T, Li WC, Dai LM, et al. Highly luminescent carbon nanodots by microwave-assisted pyrolysis. Chem Commun 2012;48:7955-7.
[28] Jaiswal A, Ghosh SS, Chattopadhyay A. One step synthesis of C-dots by microwave mediated caramelization of poly(ethylene glycol). Chem Commun 2012;48:407-9.
[29] Puvvada N, Kumar BNP, Konar S, Kalita H, Mandal M, Pathak A. Synthesis of biocompatible multicolor luminescent carbon dots for bioimaging applications. Sci Technol Adv Mater 2012;13.
[30] Qin XY, Lu WB, Asiri AM, Al-Youbi AO, Sun XP. Microwave-assisted rapid green synthesis of photoluminescent carbon nanodots from flour and their applications for sensitive and selective detection of mercury(II) ions. Sensor Actuat B-Chem 2013;184:156-62.
[31] Dey S, Chithaiah P, Belawadi S, Biswas K, Rao CNR. New methods of synthesis and varied properties of carbon quantum dots with high nitrogen content. J Mater Res 2014;29:383-91.
[32] Hu Q, Paau MC, Zhang Y, Gong XJ, Zhang L, Lu DT, et al. Green synthesis of fluorescent nitrogen/sulfurdoped carbon dots and investigation of their properties by HPLC coupled with mass spectrometry. RSC Adv 2014;4:18065-73.
[33] Liu Y, Xiao N, Gong NQ, Wang H, Shi X, Gu W, et al. One-step microwave-assisted polyol synthesis of green luminescent carbon dots as optical nanoprobes. Carbon 2014;68:258-64.
[34] Wang W, Li YM, Cheng L, Cao ZQ, Liu WG. Water-soluble and phosphorus-containing carbon dots with strong green fluorescence for cell labeling. J Mat Chem B 2014;2:46-8.

[35] Zhao Q-L, Zhang Z-L, Huang B-H, Peng J, Zhang M, Pang D-W. Facile preparation of low cytotoxicity fluorescent carbon nanocrystals by electrooxidation of graphite. Chem Commun 2008:5116-8.
[36] Hu SL, Liu J, Yang JL, Wang YZ, Cao SR. Laser synthesis and size tailor of carbon quantum dots. J Nanopart Res 2011;13:7247-52.
[37] Sachdev A, Matai I, Gopinath P. Implications of surface passivation on physicochemical and bioimaging properties of carbon dots. RSC Adv 2014;4:20915-21.
[38] Liu MY, Zhang XQ, Yang B, Deng FJ, Ji JH, Yang Y, et al. Luminescence tunable fluorescent organic nanoparticles from polyethyleneimine and maltose: facile preparation and bioimaging applications. RSC Adv 2014;4:22294-8.
[39] Geiger J Aneja MK, Rudolph C. Vectors for pulmonary gene therapy. Int J Pharm 2010;390:84-8.
[40] Beck-Broichsitter M, Merkel OM, Kissel T. Controlled pulmonary drug and gene delivery using polymeric nano-carriers. J Control Release 2012;161:214-24.
[41] van Rijt SH, Bein T, Meiners S. Medical nanoparticles for next generation drug delivery to the lungs. Eur Respir J 2014;44:365-74.
[42] Densmore CL, Orson FM, Xu B, Kinsey BM, Waldrep JC, Hua P, et al. Aerosol delivery of robust polyethyleneimine-DNA complexes for gene therapy and genetic immunization. Mol Ther 2000;1:180-8.
[43] Davies LA, McLachlan G, Sumner-Jones SG, Ferguson D, Baker A, Tennant P, et al. Enhanced lung gene expression after aerosol delivery of concentrated pDNA/PEI complexes. Mol Ther 2008;16:1283-90.
[44] Alton E, Stern M, Farley R, Jaffe A, Chadwick SL, Phillips J, et al. Cationic lipid-mediated CFTR gene transfer to the lungs and nose of patients with cystic fibrosis: a double-blind placebo-controlled trial. Lancet 1999;353:947-54.
[45] McLachlan G, Davidson H, Holder E, Davies LA, Pringle IA, Sumner-Jones SG, et al. Pre-clinical evaluation of three non-viral gene transfer agents for cystic fibrosis after aerosol delivery to the ovine lung. Gene Ther 2011;18:996-1005.
[46] Alton E, Boyd AC, Cheng SH, Davies JC, Davies LA, Dayan A, et al. Toxicology study assessing efficacy and safety of repeated administration of lipid/DNA complexes to mouse lung. Gene Ther 2014;21:89-95.
[47] Saltzman WM, Radomsky ML, Whaley KJ, Cone RA. Antibody diffusion in human cervical-mucus. Biophys J 1994;66:508-15.
[48] Olmsted SS, Padgett JL, Yudin AI, Whaley KJ, Moench TR, Cone RA. Diffusion of macromolecules and virus-like particles in human cervical mucus. Biophys J 2001;81:1930-7.
[49] Lai SK, O'Hanlon DE, Harrold S, Man ST, Wang YY, Cone R, et al. Rapid transport of large polymeric nanoparticles in fresh undiluted human mucus. Proc Natl Acad Sci U S A 2007;104:1482-7.
[50] Schuster BS, Suk JS, Woodworth GF, Hanes J. Nanoparticle diffusion in respiratory mucus from humans without lung disease. Biomaterials 2013;34:3439-46.
[51] Ikeda Y, Nagasaki Y. Impacts of PEGylation on the gene and oligonucleotide delivery system. J Appl Polym Sci 2014;131:10.
[52] Wattendorf U, Merkle HP. PEGylation as a tool for the biomedical engineering of surface modified microparticles. J Pharm Sci 2008;97:4655-69.

Efficient in vitro and in vivo pulmonary delivery of nucleic acid by carbon dot-based nanocarriers

Philippe Pierrat, Rongrong Wang, Dimitri Kereselidze, Marie Lux, Pascal Didier, Antoine Kichler, Françoise Pons, and Luc Lebeau

Figure 1. Size distribution (by number) of pristine CD as a function of irradiation time at fixed power output of the microwave oven (700 W).

Figure 2. Transmission electron micrographs of the purified carbon dots. Inset: size distribution of the particles as determined by DLS (X-axis: particle size in nm; Y-axis: particle number in %). The samples were negatively stained with 1 % uranyl acetate: a) **CD-4**, b) **CD-5**, c) **CD-6**, d) **CD-7**, e) **CD-8**, f) **CD-9**. Scale bar: 100 nm.

Figure 3. Absorbance and photoluminescence emission spectra with increasing excitation wavelength (in 10 nm increments, starting from 390 nm) of **CD-7**. The emission spectral intensities are normalized in the inset.

Figure 4. Absorbance and photoluminescence emission spectra (right, $\lambda_{exc.}$ = 360 nm) of carbon dots **CD-4** to **CD-7** prepared under various energy supply regimes (a and b, resp.), and of those prepared varying the w/w reactant ratio, **CD-7** to **CD-9** (c and d, resp.). The samples were prepared in ultrapure water (0.50 mg/mL).

Figure 5. Expression of luciferase (*left*) and LDH release (*right*) in A549 cells treated with pCMV-FLuc pDNA complexed with carbon dots **CD-4** (a), **CD-7** (b) or **CD-8** (c), or with bPEI25k (d). Complexes were prepared at various carrier/DNA weight ratios (0.5 to 32) and the assays were carried out with increasing DNA concentration (0.2, 0.4, and 0.8 µg/well), in the presence of 10 % FBS. Control (C) refers to basal bioluminescence measured in untreated cells. In the LDH release assay, basal LDH measured in untreated cells is set at 0 %, and 100 % represents the total LDH released after cell lysis of these control cells. Data shown are representative of a triplicate determination (mean ± SD).

Figure 6. Cytotoxicity of **CD-7** and its complexes with pDNA, and comparison with bPEI25k and the subsequent polyplexes, after incubation of A549 cells for 24 h. Mitochondrial activity as measured by the MTT assay (a) and LDH release (b) from cells treated with various concentrations of the carriers (**CD-7**: plain line, bPEI25k: dashed line). Mitochondrial activity (c) and LDH release (d) from cells treated with **CD-7**/pCMV-FLuc (w/w = 2.6; plain line) or bPEI25k/pCMV-FLuc complexes (w/w = 1.3; dashed line). Basal mitochondrial activity measured in untreated cells is set at 100 %. Basal LDH measured in untreated cells is set at 0 %, and 100 % corresponds to LDH released after complete cell lysis of control (untreated) cells. Data shown correspond to triplicate determinations (mean ± SD).

Figure 7. Inhibition of FLuc gene expression in A549-Luc cells by **CD-7**/siRNA and bPEI25k/siRNA. Each carrier was formulated with either untargeting siRNA (sic: *grey*) or

Luciferase-targeting siRNA (siLuc: *black*), varying the carrier/siRNA weight ratio (final siRNA concentration in the wells: 50 nM). Luciferase activity (RLU/mg protein) was measured at the end of a 48-h incubation period and plotted relative to untreated cells (100 % Luciferase expression, data not shown). Data are representative of a triplicate determination (mean ± SD).

Figure 8. Cellular imaging of **CD-7**/DNA-Cy5 complexes in A549 cells. Cells were incubated for various periods of time (1, 4, and 24 h). (**a**) λ_{ex} = 488 nm (NR12S); (**b**) λ_{ex} = 405 nm (**CD-7**); (**c**) λ_{ex} = 635 nm (DNA-Cy5); (**d**) merged images (all scale bars: 10 µm).

Figure 9. Cellular imaging of **CD-7**/siRNA-Cy5 complexes in A549 cells. Cells were incubated for various periods of time (1, 4, and 24 h). (**a**) λ_{ex} = 488 nm (NR12S); (**b**) λ_{ex} = 405 nm (**CD-7**); (**c**) λ_{ex} = 635 nm (DNA-Cy5); (**d**) merged images (all scale bars: 10 µm).

Figure 10. GLuc expression after non-viral gene transfer to mouse lungs. Carrier/pCMV-GLuc complexes (40 µg pDNA in 50 µL) were administered to mice at the indicated w/w ratio by intranasal instillation and *Gaussia* Luciferase expression was quantified in lung homogenates 24 h after transfection (n = 4/group) as described in the Materials and methods section. Negative control mice (C) received pure water (50 µL). *Complexes were prepared according to procedure B (see Materials and methods section).

Figure 11. KC concentration in bronchoalveolar lavage fluids from mice treated with the carrier/DNA complexes. Carrier/pCMV-GLuc complexes (40 µg pDNA in 50 µL) were administered to mice at the indicated w/w ratio by intranasal instillation. Broncoalveolar lavage fluids were collected at 24 h after transfection (n = 4/group) as described in the Materials and methods section. Negative control mice (C) received pure water (50 µL). *Complexes were prepared according to procedure B (see Materials and methods section).

Efficient in vitro and in vivo pulmonary delivery of nucleic acid by carbon dot-based nanocarriers

Philippe Pierrat, Rongrong Wang, Dimitri Kereselidze, Marie Lux, Pascal Didier, Antoine Kichler, Françoise Pons, and Luc Lebeau

Table 1. Dialysis efficiency of a CA-bPEI25k mixture under various pH conditions. The amount of residual material in the dialysis device is indicated in % (w/w).

Membrane (MWCO, Da)	**pH**			
	1	2	7	13
3.500	5.9	20.0	22.3	4.9
1.000	9.1	–	27.9	–

CA (0.50 g) and bPEI25k (0.25 g) in 5 mL ultrapure water were dialyzed for 24 h against ultrapure water at the indicated pH (adjusted through addition of conc. HCl or NaOH solution). Dialysate was changed at time points 2, 6, and 12 h. Then dialysate was replaced with ultrapure water and dialysis was continued for 48 h (dialysate was changed every 12 h) before the samples were collected and lyophilized.

Table 2. Influence of pH on the preparation of CD under microwave radiation.

Sample	**pH**	**Size** (nm)	ζ (mV)	**Fluorescence** (a.u.)
CD-1	1	8.7 ± 4.0	+ 36.5 ± 6.2	1.51
CD-2	4	15.7 ± 14.6	+ 51.8 ± 4.8	1.21
CD-3	8	18.2 ± 8.3	+ 2.7 ± 4.4	0.09

A mixture of CA (0.50 g) and bPEI25k (0.25 g) was solubilized in 10 mL ultrapure water at the indicated pH, and was irradiated for 4 min at 700 W. CD were purified by dialysis before analysis. Fluorescence intensity at 450 nm was measured for sample in water (0.50 mg/mL; λ_{exc} = 360 nm).

Table 3. Influence of the microwave irradiation regime on the properties of the carbon dots prepared from a mixture of CA (0.50 g) and bPEI25k (0.25 g) in HCl 0.1 N (5 mL). Carbon dots were purified by dialysis before analysis and yield refers to purified carbon dots (with respect to 0.75 g of starting material, *i.e.* 100 %). Particle zeta potential and size were measured in NaCl 1.5 mM. Fluorescence intensity was measured for samples in water (0.50 mg/mL).

Sample	**MW regime**		**Size** (nm)	**ζ** (mV)	**Fluorescence** (a.u.)	**Φ (%)**	**Yield** (%)
	Power (W)	**Time** (s)					
CD-4	100	1050	12.0 ± 1.0	+ 66.3 ± 4.8	0.1	48.1	31.8
CD-5	300	350	13.2 ± 1.3	+ 46.9 ± 9.9	1.2	42.6	27.7
CD-6	450	233	12.9 ± 3.0	+ 43.1 ± 8.5	3.2	38.9	20.7
CD-7	700	150	19.7 ± 1.1	+ 42.1 ± 6.2	3.7	31.5	20.0

Table 4. Influence of the stoichiometry of the reactants on the physical and photophysical properties of the resulting carbon dots. Samples were prepared from 0.5 g CA and the indicated amount (w/w) of bPEI25k in HCl 1N (5 mL), under microwave radiation for 150 s (power output 700 W). Particle zeta potential and size were measured in NaCl 1.5 mM. Intensity of fluorescence emission was measured for samples in water (0.50 mg/mL). Yield refers to purified carbon dots.

Sample	**bPEI25k** (%)	**Size** (nm)	**ζ** (mV)	**Fluorescence** (a.u.)	**Φ** □□□	**Yield** (%)
CD-8	20	21.1 ± 3.9	+ 61.5 ± 11.6	11.1	35.0	22.4
CD-7	33	19.7 ± 1.1	+ 42.1 ± 6.2	3.7	31.5	20.0
CD-9	50	24.9 ± 2.1	+ 57.1 ± 15.3	1.0	28.0	30.8

Table 5. Size and ζ potential of the DNA complexes with **CD-7** at various CD/DNA ratios (w/w).

w/w	**Size** (nm)	**ζ** (mV)
0.5	88.7 ± 1.4	-20.5 ± 4.6
1	41.7 ± 5.0	+5.0 ± 1.3
2	35.1 ± 1.3	+15.5 ± 1.7
4	32.7 ± 4.0	+18.5 ± 4.2
8	27.8 ± 3.8	+17.0 ± 7.6
16	26.1 ± 4.0	+20.2 ± 2.8
32	20.6 ± 3.5	+24.3 ± 2.0

Table 6. Size and ζ potential of the pCMV-GLuc complexes with GL67A, PEI, and **CD-7** at various CD/DNA ratios (w/w).

Carrier	**w/w**	**Size** (nm)	ζ (mV)
GL67A	–	180.2 ± 13.4	– 32.5 ± 1.0
bPEI25k	1.3	320.3 ± 114.0	+ 18.1 ± 1.7
CD-7	1.6*	171.9 ± 2.1	+ 37.9 ± 0.2
"	2.1*	57.3 ± 1.1	+ 34.4 ± 3.3
"	2.6*	48.6 ± 0.3	+ 50.1 ± 7.0
"	2.6	205.3 ± 30.6	+ 27.3 ± 0.6
"	3.1	181.7 ± 59.4	+ 27.7 ± 0.5
"	3.6	199.1 ± 3.9	+ 29.3 ± 0.4

*The samples were prepared through concentration of diluted CD/DNA complexes (protocol B, see Material and methods).

Figure

Click here to download Figure: 9-Pierrat Figure.pdf

Figure 1

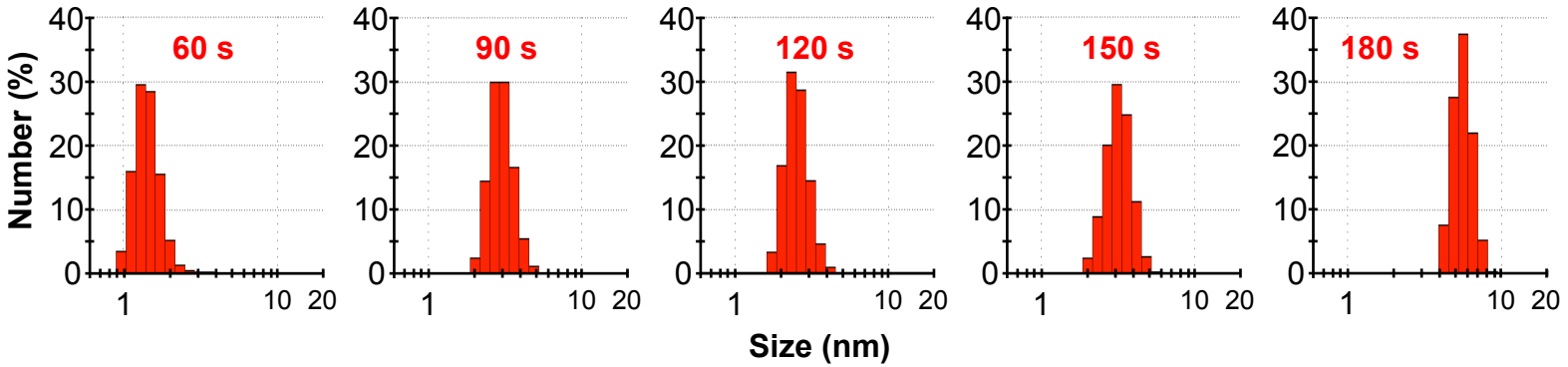

Figure 2

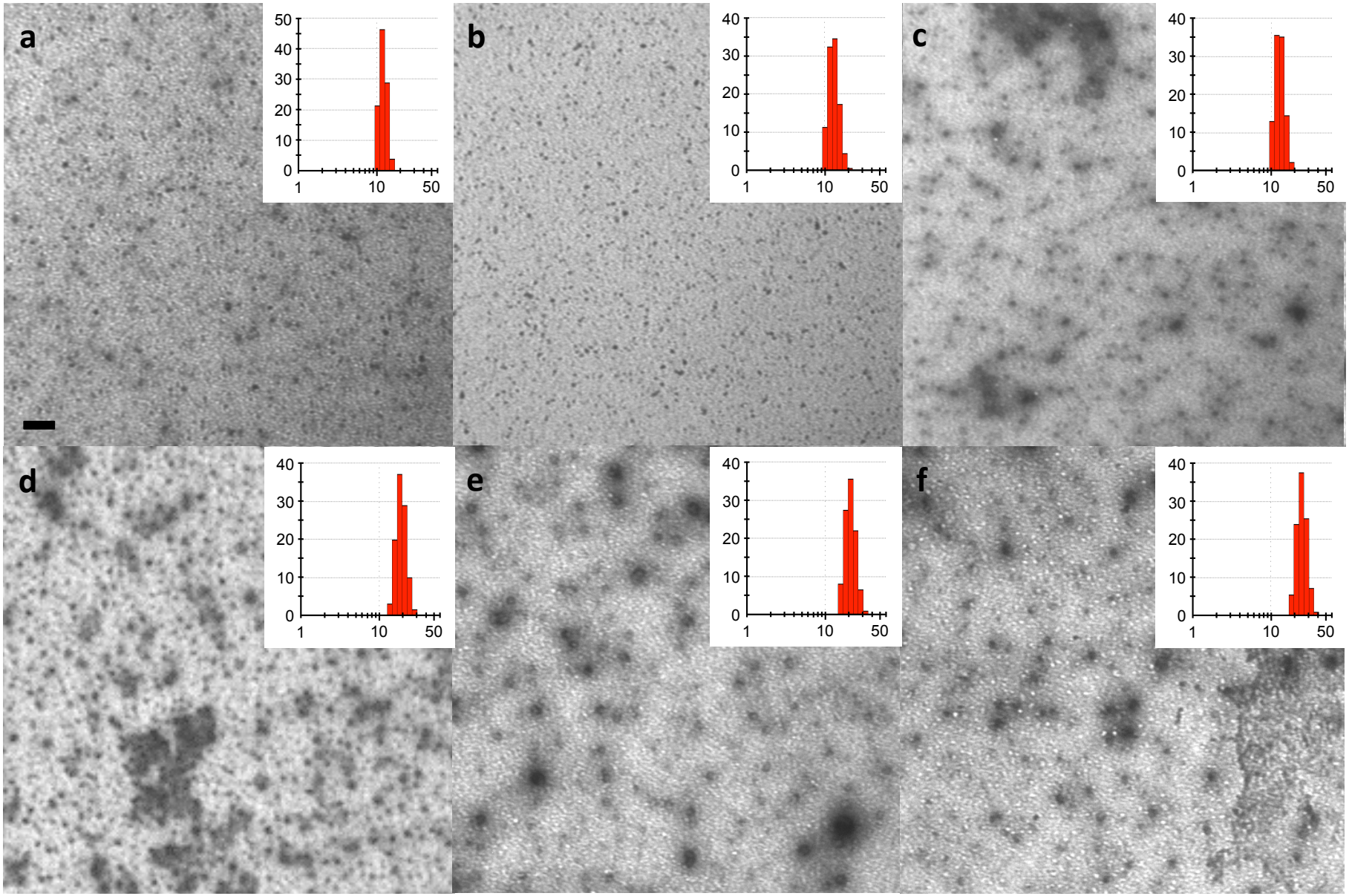

Figure 3

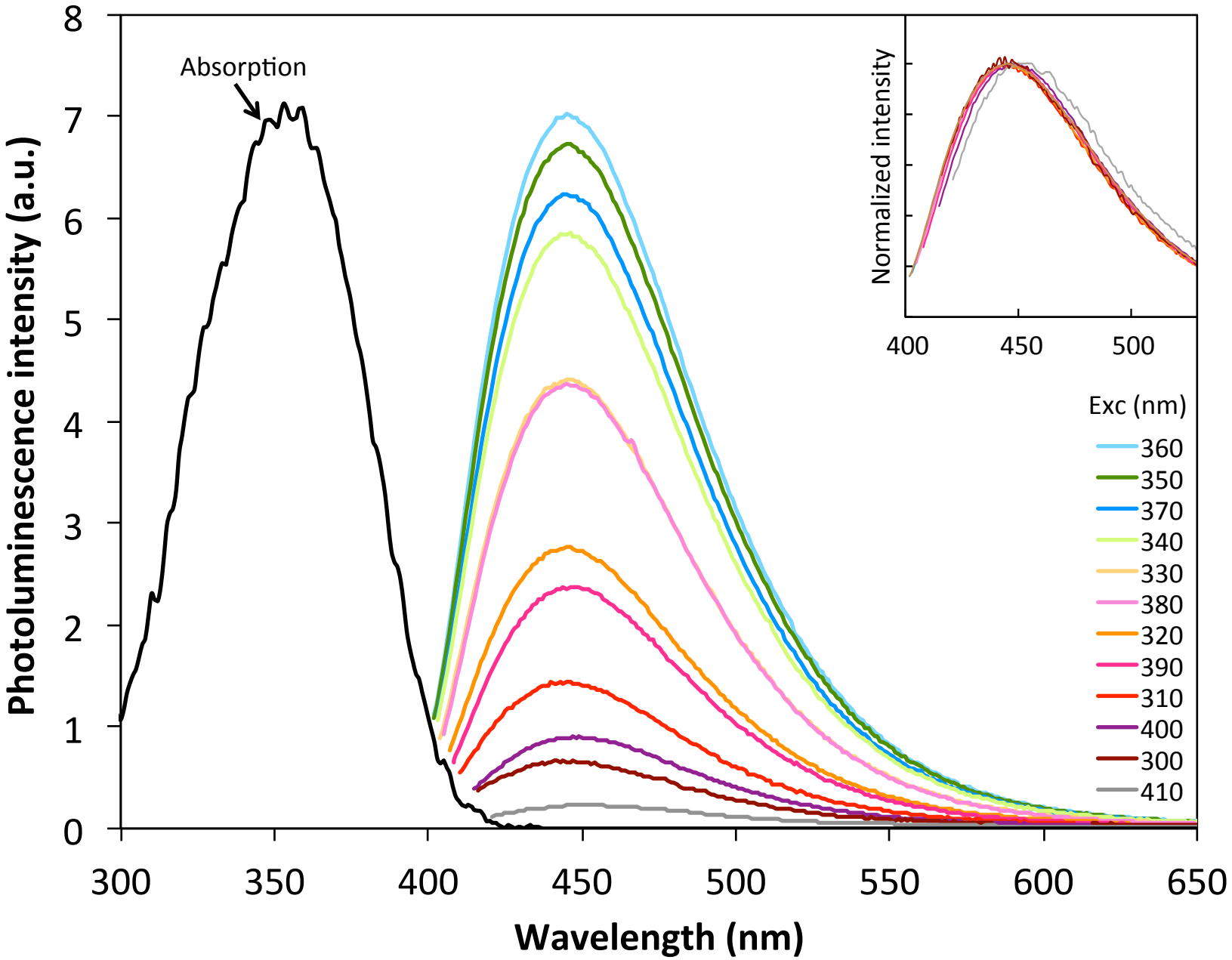
Absorption
Photoluminescence intensity (a.u.)
Wavelength (nm)
0
1
2
3
4
5
6
7
8
300
350
400
450
500
550
600
650
Normalized intensity
400
450
500
Exc (nm)
360
350
370
340
330
380
320
390
310
400
300
410

Figure 4

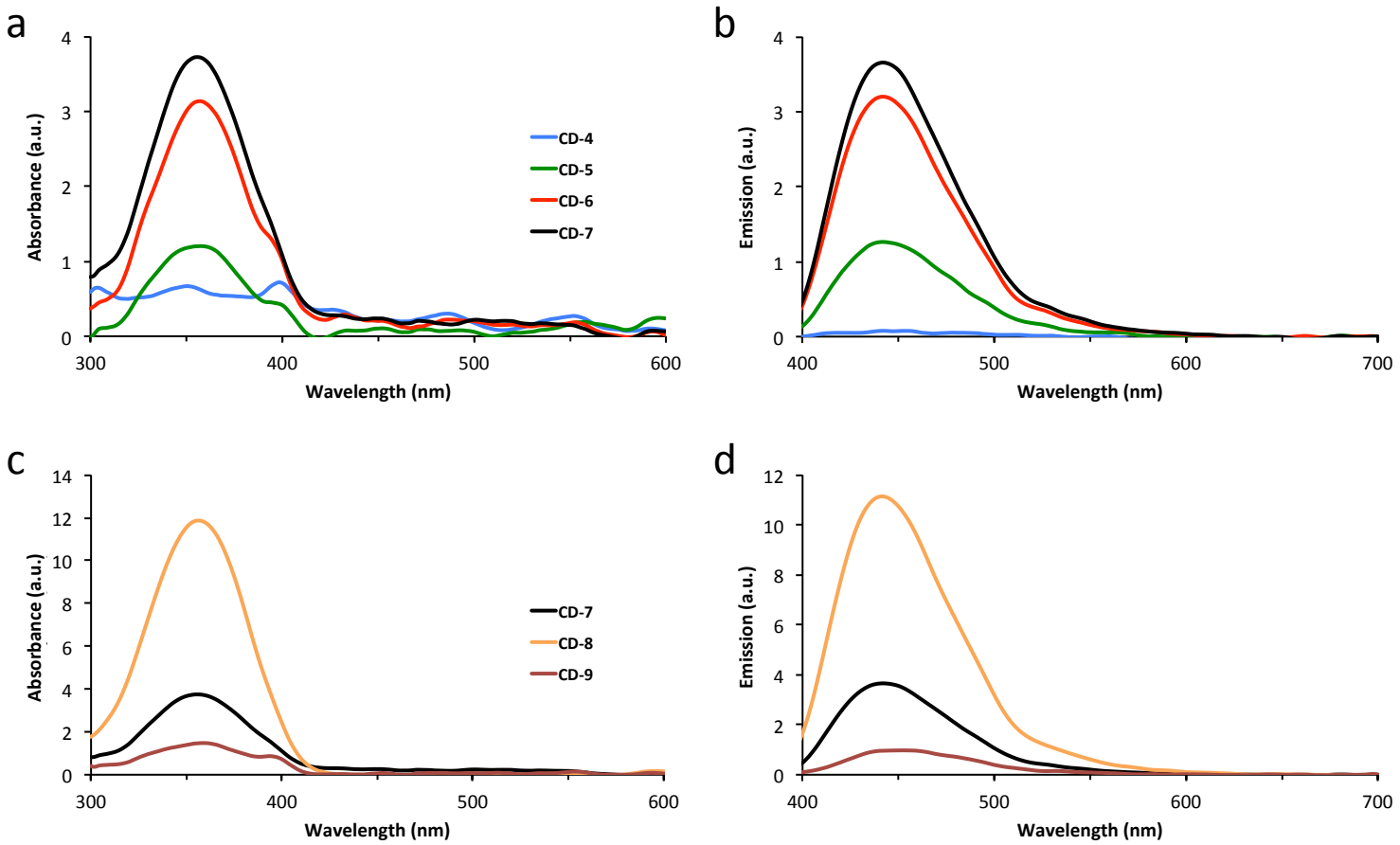
a
Absorbance (a.u.)
Wavelength (nm)
CD-4
CD-5
CD-6
CD-7
b
Emission (a.u.)
Wavelength (nm)
c
Absorbance (a.u.)
Wavelength (nm)
CD-7
CD-8
CD-9
d
Emission (a.u.)
Wavelength (nm)

Figure 5

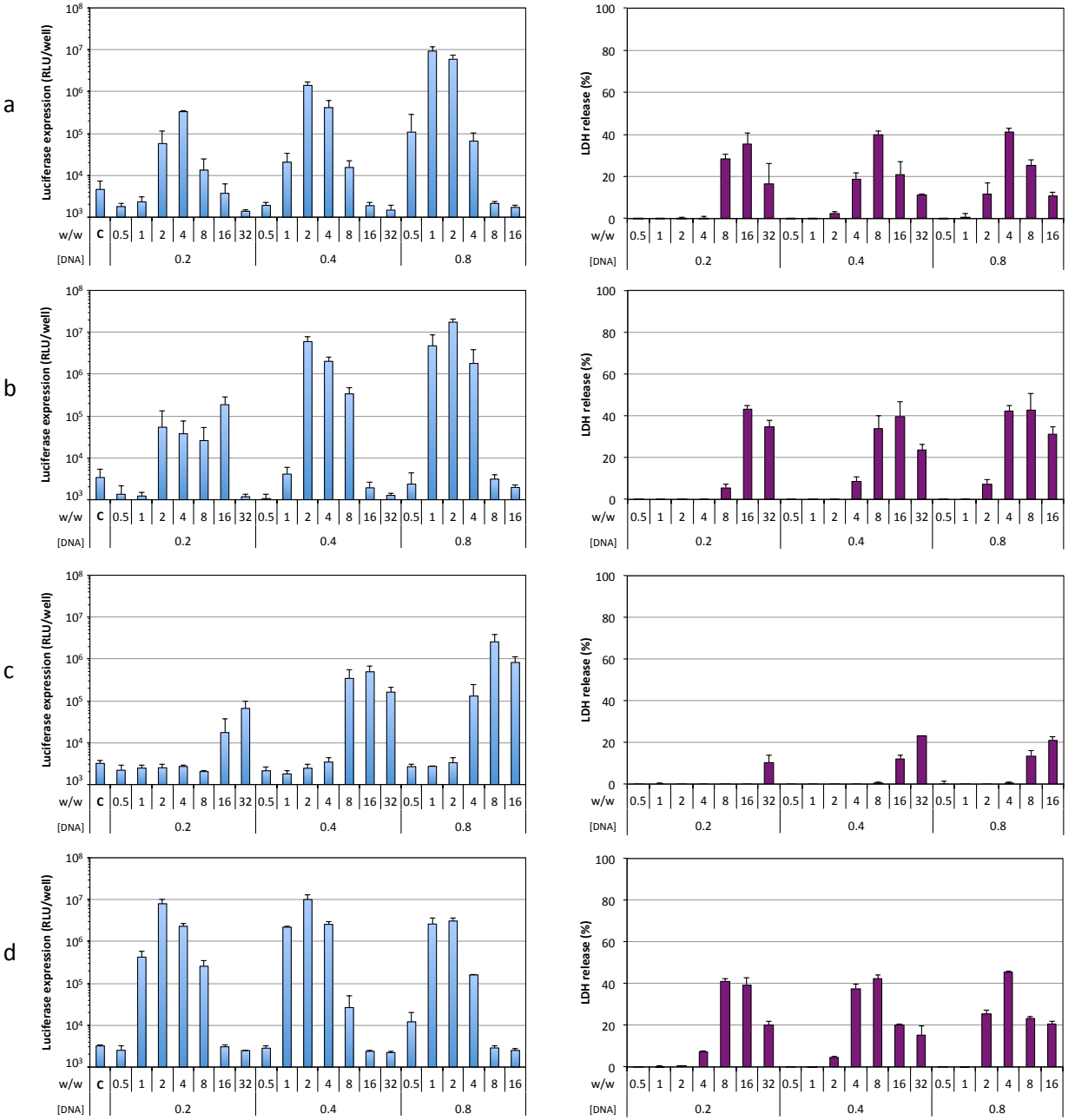
a
b
c
d
Luciferase expression (RLU/well)
LDH release (%)
w/w
[DNA]
C
0.5 1 2 4 8 16 32 0.5 1 2 4 8 16 32 0.5 1 2 4 8 16
0.2
0.4
0.8

Figure 6

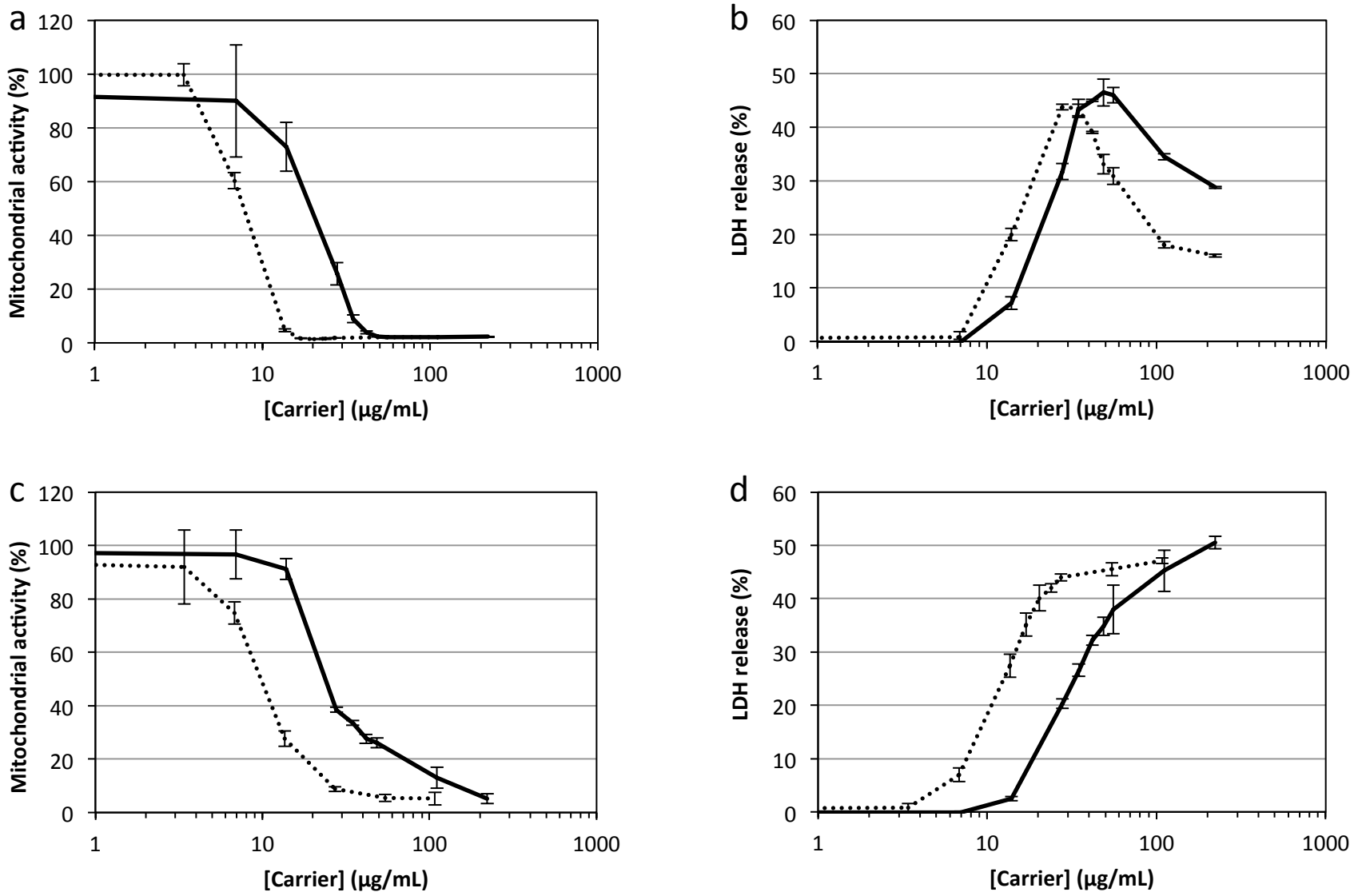
a
Mitochondrial activity (%)
120
100
80
60
40
20
0
1
10
100
1000
[Carrier] (µg/mL)
b
LDH release (%)
60
50
40
30
20
10
0
1
10
100
1000
[Carrier] (µg/mL)
c
Mitochondrial activity (%)
120
100
80
60
40
20
0
1
10
100
1000
[Carrier] (µg/mL)
d
LDH release (%)
60
50
40
30
20
10
0
1
10
100
1000
[Carrier] (µg/mL)

Figure 7

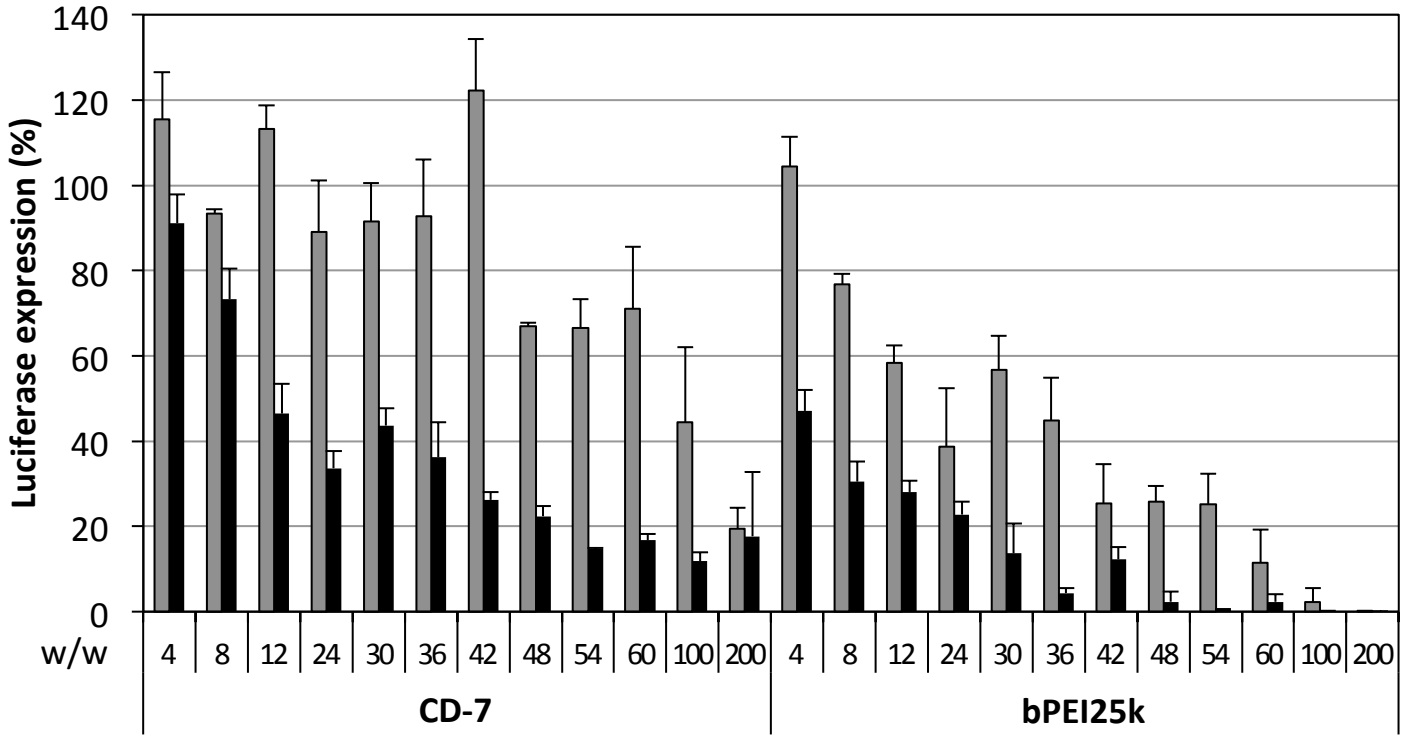
Luciferase expression (%)
140
120
100
80
60
40
20
0
w/w
4
8
12
24
30
36
42
48
54
60
100
200
CD-7
bPEI25k

Figure 8

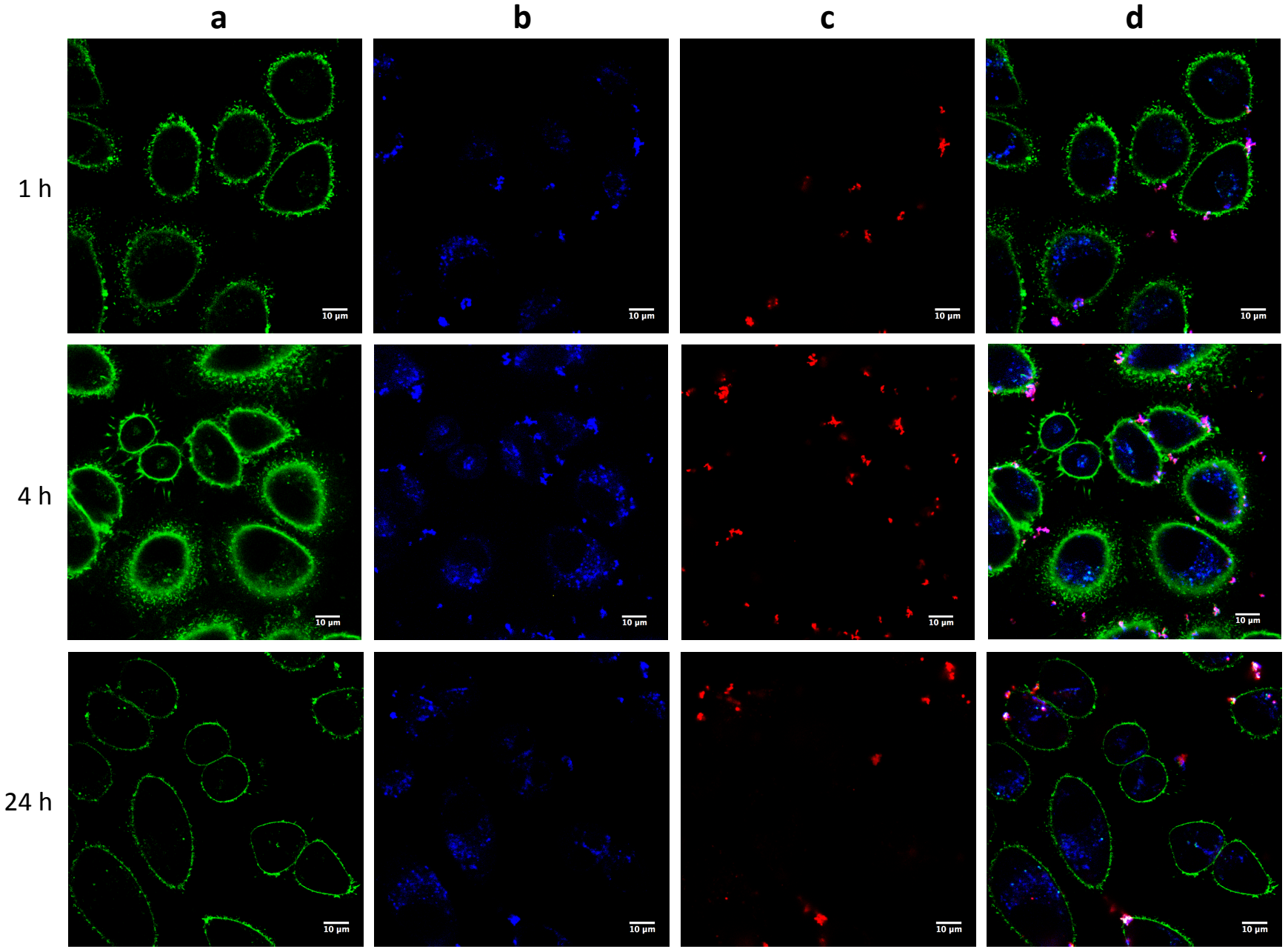

Figure 9

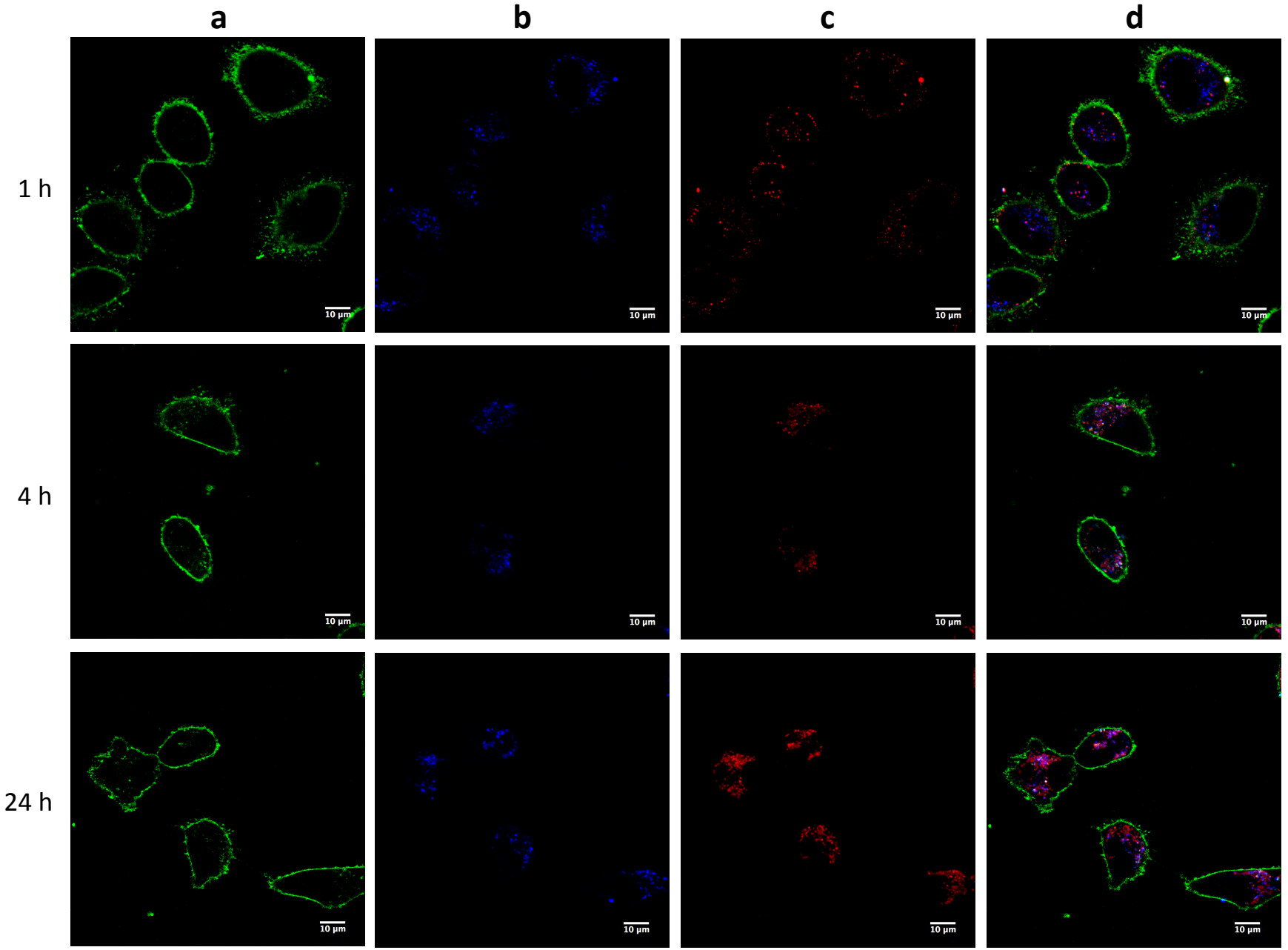

Figure 10

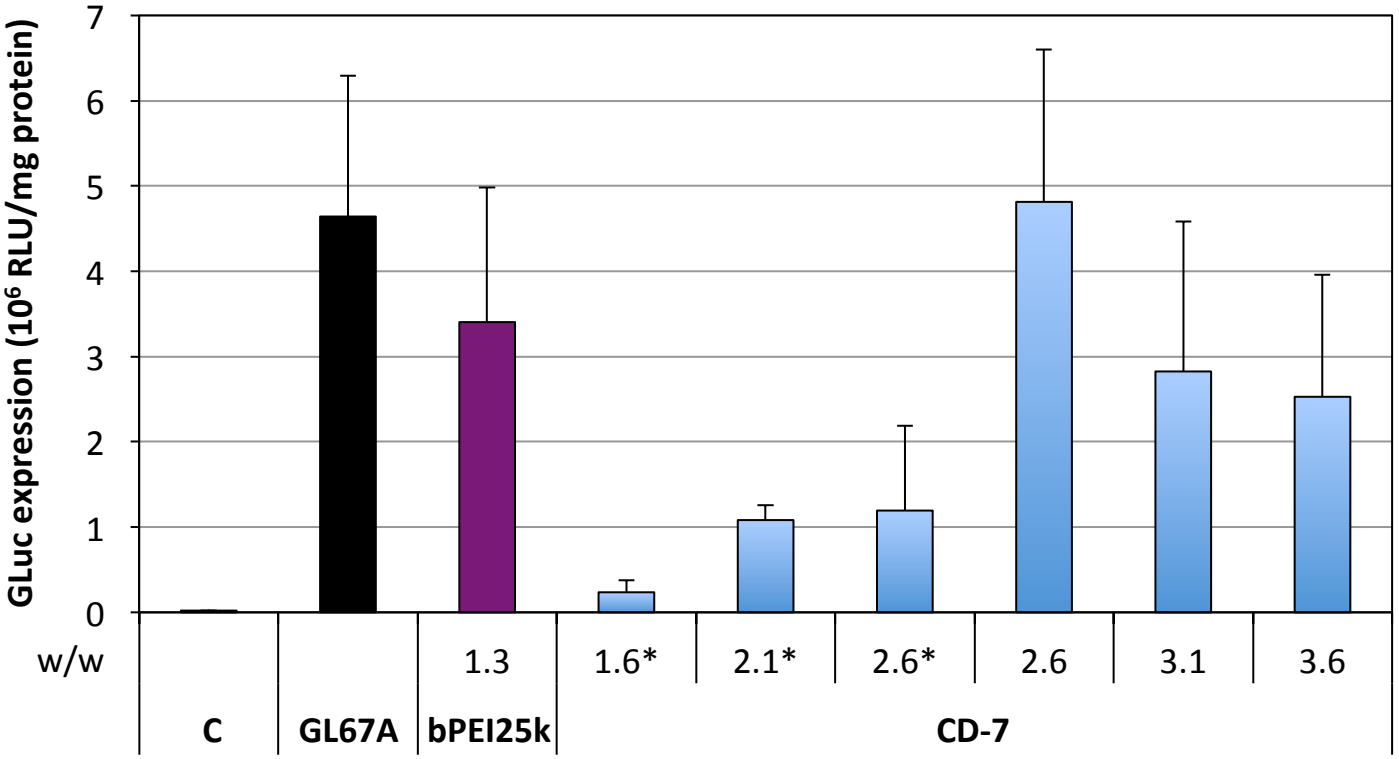
GLuc expression (10^6 RLU/mg protein)
7
6
5
4
3
2
1
0
w/w
1.3
1.6*
2.1*
2.6*
2.6
3.1
3.6
C
GL67A
bPEI25k
CD-7

Figure 11

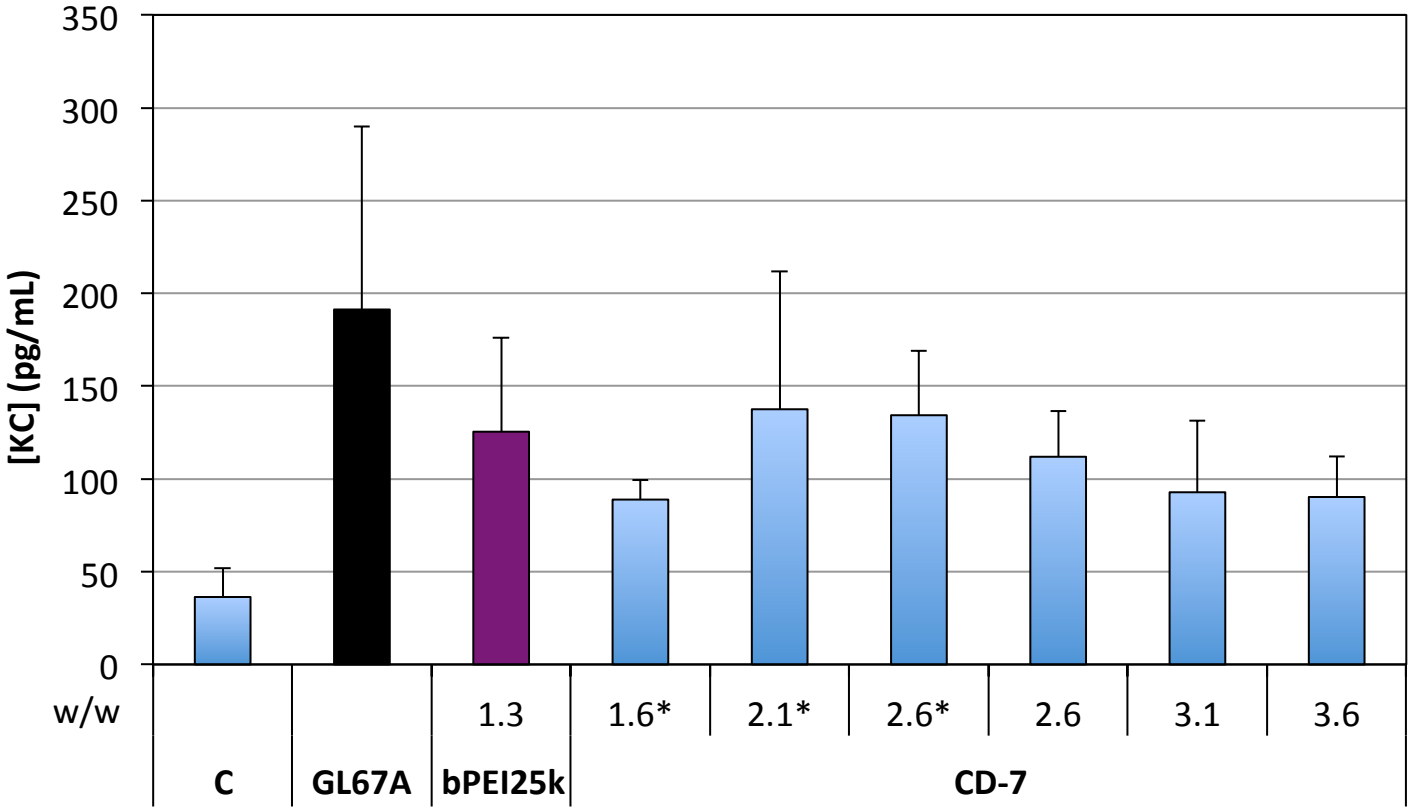
350
300
250
200
150
100
50
0
[KC] (pg/mL)
w/w
1.3
1.6*
2.1*
2.6*
2.6
3.1
3.6
C
GL67A
bPEI25k
CD-7

Supplementary Files

Click here to download Supplementary Files: 10-Pierrat SI.pdf